11- AMINO-1 UNDECENE - COVERED SI (100) AND GE (100) SURFACES

_____

A Dissertation

presented to

the Faculty of the Graduate School

at the University of Missouri-Columbia

_____

In Partial Fulfillment

of the Requirements for the Degree

Master of Science

_____

by

JING LIU

Dr. C. Michael Greenlief, Thesis Supervisor

MAY 2012

The undersigned, appointed by the Dean of the Graduate School, have examined the dissertation entitled

11- AMINO-1 UNDECENE - COVERED SI (100) AND GE (100) SURFACES

Presented by Jing Liu,

A candidate for the degree Master of Science,

And hereby certify that, in their opinion, it is worthy of acceptance.

Professor C. Michael Greenlief

Professor Gary A. Baker

Professor Haskell Taub

Dedicated to my daughter Caroline, my husband Zhengxin and my parents.

ACKNOWLEDGEMENTS

I would like to thank my supervisor, Professor C. Michael Greenlief, for his guidance and great advice throughout these years. My research and dissertation could not be done without his encouragement and strong support. I also would like to thank all of my committee members: Professor Gary A. Baker and Professor Haskell Taub, for their advice and comments. Many thank goes to the University of Missouri-Columbia for granting me the opportunity to study in the chemistry department and for their funding though teaching assistantships.

I would like to acknowledge Dr. Wei Wycoff, for helping me on the NMR techniques and Dr. Nathan D. Leigh for his mass spectrometry support. Thanks to all of chemistry department staff, especially, Jerry Brightwell for his assistance and great patience.

I would like to thank my dear parents and my husband for their moral support all these years.

I would like to thank all my friends I have made here for their support, comfort and encouragement.

TABLE OF CONTENTS

Chapter 2: Experimental section

Chapter 3: Results and Discussion

LIST OF FIGURES

LIST OF TABLES

11- AMINO-1 UNDECENE - COVERED SI (100) AND GE (100) SURFACES

Jing Liu

Dr. C. Michael Greenlief, Thesis Supervisor

ABSTRACT

Due to the similar properties and structures of silicon and germanium surfaces, they have similar methods of passivation and organic functionalizaiton reactions. The formation of organic monolayers on semiconductor surfaces has recently become an area of intense investigation. One important motivation is the need to control electronic properties by covalently attaching molecules to the semiconductor surface. Another driving motivation is to incorporate organic molecular properties, such as chemical affinity, flexibility, conductivity, and chirality for developing biomedical sensors.

The research described herein investigates the hydrogen, t-BoC, and amine terminated Si(100) or Ge(100) surfaces, and to determine the elemental percentages of carbon, nitrogen, oxygen and silicon/ germanium present at the semiconductor surface using X-ray photoelectron spectroscopy (XPS).

Chapter 1: Introduction

1.1 Background

Group IV semiconductor materials, including Si and Ge, play an increasingly important role in many modern technology fields. In addition to playing a crucial role in integrated circuits, modification of semiconductor surfaces, especially silicon substrates, with ultrathin organic films to allow for meaningful interaction with biological targets has been intensively studied in recent years. These structures are very important for the development of silicon-based bioelectrical sensors and devices[1,2], nanoparticle probes[3,4], nanowire sensors[5], photonic devices[6,7], cantilever sensors[8,9], microarrays[10,11], microfluidic[12] and silicon - neuron interfaces[13].

Over the past 40 years, silicon is considered to be the best choice of semiconductor for transistors and integrated circuits. The choice of silicon over the other semiconductors is that it easily exists as an oxide, SiO_2, in ambient environment, and the oxide has a function to passivate the silicon and form a defect- free interface between the Si and SiO_2. The interface formed naturally between Si and SiO_2 is critical to the operation of the transistor, as the interface between the dielectric layer and the semiconductor plays a significant role in determining the electrical properties of the device. However, as the size of microelectronic devices continues to decrease, it becomes increasingly more important to understand the mechanism of integrating molecular systems with semiconductor surfaces. In order to integrate biological

molecules with microelectronics, the stability of the semiconductor interface is crucial to performance.

Organic monolayers provide an opportunity to overcome many barriers that hindered the specific integration of microelectronics with organic and biological systems[1]. Thin monolayers can have specific electrical, mechanical, or optical functions, which depend on the nature of the bonding within the layers. For example, monolayers composed of alkyl chains can act as barriers to aqueous environments due to the chains' hydrophobic properties.

Here, I will present the properties and structures of silicon and germanium surfaces, methods of passivation, organic functionalizaiton reactions on semiconductor surfaces and X-ray Photoelectron Spectroscopy characterization.

1.1.1 Properties of semiconductor

With the trend of continually shrinking dimensions for transistors, a shift away from SiO_2 to other dielectric materials is being sought. At the nanometer-scale dielectric thicknesses used today, it is important to find a better alternative material with a larger dielectric constant than SiO_2. At these very short distances, the influence of leakage currents caused by electron tunneling through the dielectric will impede device performance. The possible elimination of SiO_2 from some of the core structures of an integrated circuit is leading to the study of other semiconductor materials for device fabrication. In fact, it has been known that other semiconductors, (for example, germanium and GaAs) have better inherent electrical properties than Si.

Ge has chemical properties that are similar to silicon and, it is the reason for examing organic monolayers on germanium surfaces. The mobility of germanium exceeds that of silicon by a factor of three[14,15], providing an advantage for high- speed circuits. In addition, much of the processing of Ge can be conducted at lower temperatures compared to Si; part of which is due to a lower melting point for Ge (1210K) versus Si (1683K)[16]. Thirdly, the lattice parameters of Ge are close to those of GaAs, providing the possibility of integration of GaAs on to Ge-based chips. Finally, the preparation and passivation methods of germanium surfaces are analogous to those used for silicon studied.

1.1.2 Structures of semiconductor

The crystal structures of silicon that are used most industrially are Si(100), Si(011), and Si(111). Si(100) is the orientation used most often. The similarity between Si(100) and Ge(100) will be discussed below as these are the structures used in this thesis. In the crystalline state, silicon[17], germanium[18] and carbon (diamond) [19-22], are covalent solids that form a diamond cubic lattice structure. Each of these crystalline materials exhibit similar surface reconstructions. It is convenient to recall the geometry of the ideal unreconstructed surface. For example, atoms in the topmost four layers of the ideal Si(100) surface[17] are arranged as shown in Figure 1(a). Silicon has four valence electrons and wants to form four covalent bonds. For the ideal Si(100) surface, each surface atom has two bonds to atoms in the second layer and two non-bonding valence electrons. This situation leads to a relatively high surface free

energy. In order to lower the free energy, the surface reconstructs. In the reconstruction geometry for each of the proposed models, some or all of the non-bonding valence electrons rebond in an effort lower the free energy of the surface. In the model shown in Figure 1(b), alternate rows of surface atoms move towards each other to form pairs, thereby forming bond with half of the non-bonding electrons. In Appelbaum's comparison with experiment and theory, the re-bonding model is strongly favored over the other proposed models[17].
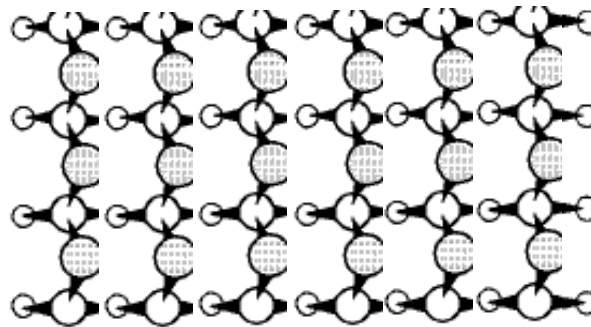
(a)
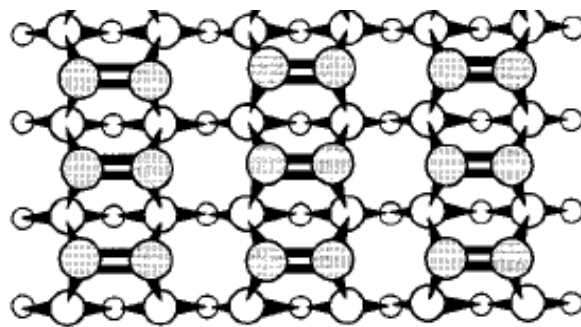
(b)
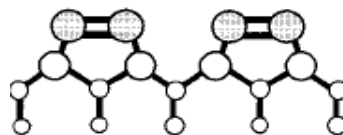
(c)
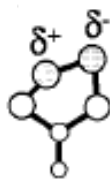
(d)

Figure 1.1:   (a) Top view of ideal unreconstructed Si (100) surface. Gray atoms represent Si=Si dimer in the topmost layer. Deeper layers are depicted with smaller circles. (b) Top view of reconstructed Si (100) surface. (c) Side view of reconstructed Si (100) surface. Surface dimers are depicted in gray. (d) Zwitterionic character of titled Si=Si dimer.
(R.J. Hamers, S.K. Coulter, M.D. Ellison, J.S. Hovis, D.F. Padowitz, M.P. Schwartz, C.M. Greenlief, J.N. Russell Jr., Acc. Chem. Res. **2000**, 33 617-624.)

The (100) crystal faces of silicon and germanium exhibit similar dimers reconstructed from pairs of surfaces atoms. On Si and Ge, the bonding between the atoms in a dimer pair is often described as being somewhat akin to a double bond, containing both a strong σ-bond and a weak π-bond. As showed in Figure 1.1 (c), the covalent bonding at the surface is most easily described using the concept of Si=Si and Ge=Ge double bonds. In Si, the π-bond is significantly weaker than a C=C bond in an alkene. The weaker π-bond is due to the strained geometry at the surface for the Si and Ge atoms. For Ge, the π-bond is even weaker for Ge, and unlike a true double bond, the dimer is tilted away from a symmetric configuration at room temperature. Early studies showed that the dimers present on the Si (100) and Ge (100) surfaces are tilted and there is charge transfer from the "down" atom to the "up" atom[23], as showed in Figure 1.1 (d). The resulting buckled dimer exhibits a zwitterionic-like   property: the up Si/Ge atom is more nucleophilic, and the down Si/Ge atom is more

5

electrophilic[24]. In Figure 1.2, the symmetric dimer structure leads to a p-(2×1)

reconstruction and it designates the new periodicity of the surface atoms. However,

depending on how the members differ in the arrangement of "up" and "down" dimers

on the (2×1) backbone both in, and perpendicular to, the dimer rows, c-(4×2) or p-

(2×2) dimer reconstructions are formed. Each of these reconstructions can be

observed locally at the Si(100) or Ge (100) surfaces by scanning- tunneling

microscopy (STM)[16,17,18].
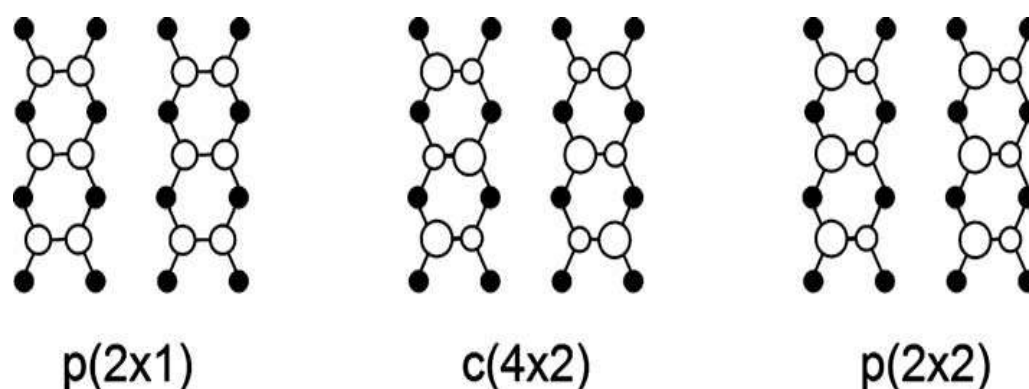
Figure 1.2: Dimer models of the Si(100) and Ge (100) surfaces. (left) p(2×1) dimer
reconstruction involving symmetric dimers: (middle) c(4×2) dimer
reconstruction with buckled dimers; and (right) p(2×2) dimer
reconstruction with buckled dimer. The open circles represent the
top-layer atoms, with the larger and smaller circles designating the up
and down atoms of the dimer respectively. The filled circles represent
the second layer of atoms.
(Loscutoff, W. P.; Bent, F. S. *Annu. Rev. Phys. Chem.* **2006**, 57,467-495.)

1.1.3 Oxidation of semiconductor surfaces

High resolution low-energy-electron loss (HREEL) spectra of oxygen adsorbed at

room temperature on clean Si or Ge(100) and (111) surfaces suggest that each oxygen

atom is doubly bonded to a surface atom[25]. Native silicon oxide (SiO_2) is a very stable passivating layer, acts as a good electrical insulator, and forms an excellent interface with Si. On the other hand, native germanium oxide (GeO_2) is water soluble, which permits contamination to reach the Ge/GeO_2 interface. The contamination is difficult to remove and GeO_2 has a poor lattice match with Ge. The instability of germanium oxide and the preparation of clean and smooth Ge surfaces, compared to silicon, have hampered the widespread use of germanium.

The most commonly used method to prepare clean germanium surfaces has been ion sputtering[26]. Ion sputtering has a number of possible disadvantages, for example, it is difficult to clean large areas, is much more time-consuming, and can result in degradation of surface smoothness.

Regarding silicon and germanium oxides, thermal oxide growth is favored for silicon, but not for germanium. For silicon, the growth of SiO_2 can be obtained from suboxides by using a high-temperature anneal[27,28], alternatively, SiO_2 can be grown directly by oxidation of a heated substrate. On the other hand, the oxidation of Ge by oxygen results in growth of Ge 1^+, 2^+ and 3^+ oxidation states, but very little of 4^+ state (GeO_2). GeO desorbs from the surface on annealing to 400 ℃ without undergoing any transformation[29].

Similar to the process of silicon cleaning, alternating cycles of wet oxide formation and etching are used to remove contaminants from the germanium surface. The commonly used oxidants are H_2O_2, HNO_3, and H_2O, in a variety of

7

concentrations[15]. Of the chemical oxidants, H_2O_2 is the most widely used[26, 30-37]. In a study by Prabhakaran and Ogino[29], GeO_x suboxide was formed instead of GeO_2 by immersing Ge (100) into the H_2O_2 solution. However, in a study by Park and co-workers, GeO_2 formation could be achieved on Ge(100) surface[38]. In the initial stage of oxidation, the Ge surface is attacked by oxidizing agents to break Ge-H and Ge-Ge bonds, and this leads to the formation of a GeO_x transition layer, followed by layer-by layer growth of GeO_2.

1.2 Passivation on semiconductor surfaces

Passivation of semiconductor surfaces is required to prevent oxidation, and to maintain surface ordering during device processing. Three different surface terminating layers are discussed below as follows: sulfide-, chloride-, and hydride-terminated Si(100) and Ge (100) surfaces.

1.2.1 Sulfide passivation

Sulfide termination on semiconductor surfaces leads to a well-passivated interface. Sulfur is bivalent and is expected to make two bonds with the surface. Because each of the surface atoms on the Ge(100) surface has two dangling bonds, sulfur may occupy the germanium lattice sites at the surface, with each Ge surface atom bonded to two sulfur atoms.
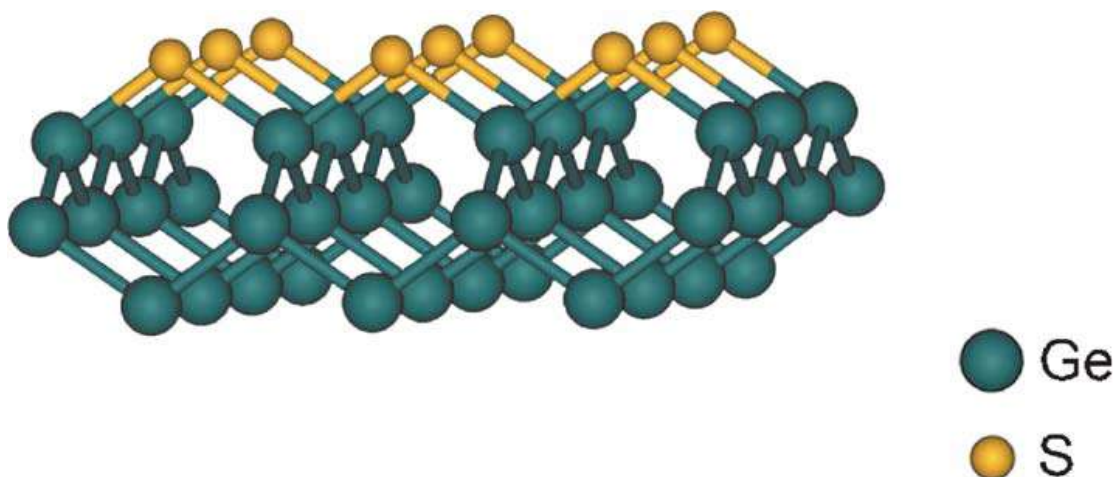
Figure 1.3:   Sulfur-terminated Ge(100) with the ideal 1×1 structure
            (Loscutoff W. P.; Bent F. S. *Annu. Rev. Phys. Chem.* **2006**, 57, 467-495.)

Several studies have investigated termination of the Ge(100) surface by an adsorbed monolayer of the group VI element[39,40]. As showed in Figure 1.3, each of the sulfur atoms can eliminate two dangling bonds, sitting in a bridge-like configuration and producing an ideal bulk (1×1) germanium structure. Such a structure could be obtained by chemisorption of elemental sulfur on the Ge(100)- 2×1 surface under ultrahigh vacuum (UHV) conditions as demonstrated by Weser and co-workers[40]. The experimental result for the adsorption of sulfur on Si(100) was reported by Kaxiras[41] and Roche, et al[42]. By considering both the chemical reactivity and induced stress inherent in the formation of a sulfide terminated Si(100) surface, Kaxiras concluded that sulfide termination was not energetically favorable for Si(100). Papageorgopoulos et al.[43,44] reported the successful room-temperature termination of the Si(100) surface by a monolayer of sulfur to form an ideal bulk Si(100)-1×1

structure, Hahn[42,45,46] et al. reported recently that they could not reproduce these results and obtained a sulfur-terminated (1×1) reconstruction structure.

Different from sulfur deposition in vacuum, the study of sulfur deposition from aqueous solution to create a bulk-terminated surface was successfully demonstrated. Anderson et al.[45] treated hydrogen-terminated Ge(100) surface with aqueous $(NH_4)_2S$ to achieve a sulfide-terminated Ge(100)-1×1 surface. Lyman[46] was also able to create a sulfide layer containing approximately two to three monolayers (ML) of sulfur by reacting clean Ge substrates with $(NH_4)_2S$ solutions.

1.2.2 Chloride passivation

The interactions of chloride with Si(100) have been extensively studied, partly because chloride etching is a key component in semiconductor device fabrication. On the surface, molecular chlorine dissociates and forms strong bonds with the Si dangling bonds. For Si(100)-2×1, surface saturation is achieved when there is one Cl atom for each Si atom. In a study by Tromp and co-workers[47], each of the first-layer Si atoms in a Cl-terminated surface are bonded to two Si atoms in the second layer, a third bond is to the other Si atom in the dimer, and the remaining bond is to Cl. Scanning tunneling microscopy (STM) data from Si (100)-2×1 confirmed this bonding configuration.
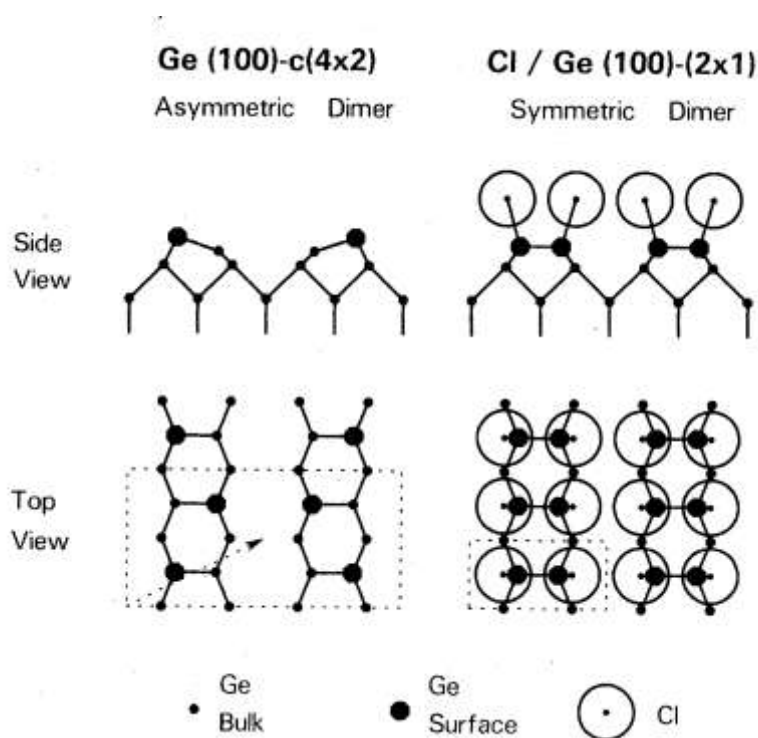
Figure 1.4: Structural models for Ge(100)-c(4×2) and Cl/Ge(100)-c(2×1). The asymmetric dimer becomes symmetric upon Cl adsorption.
(Schnell RD, Himpsel FJ, Bogen A, Rieger D, Steinmann W.*Phys. Rev. B, Condens. Matter* **1985**, 32:8052–56)

Germanium surface passivation by chloride termination inhibits oxide formation and maintains a well-ordered surface. Cullen et al.[48] first demonstrated the reaction of a Cl-terminated Ge(111) surface with ethyl-containing Grignard reagent as a means of ethylation for use in surface stabilization. In a study examining Cl adsorption on the Ge(100)-c(4×2) surface from Cl_2, Schnell and co-workers[49] observed 76% asymmetric and 24% symmetric dimers as showed in Figure 1.4. Upon forming the saturated monochloride phase, the asymmetric dimers changed to symmetric dimers. This reconfiguration is commonly observed in the adsorption of molecules on the

group IV (100) -2×1 surfaces[15]. Monochloride termination results from the addition of a chlorine atom to a dangling bond on each surface atom, in which the weak π interaction between dimer atoms breaks, and the σ-like bond character remains.

Lu[50] was the first to prepare Cl-terminated surfaces by placing a Ge(111) sample in dilute HCl solution. It is known that the strength of the Ge-Cl bond (432kJ/mol) is stronger than that of the Ge-H bond (322kJ/mol)[51]. Therefore, the formation of Ge-Cl bonds is energetically favored. The results clearly show that Cl terminates the Ge(111) surface by forming chemical bonds with dangling bonds along the Ge(111) surface normal direction. The resulting surface structure is similar to the structure formed by Cl adsorption in vacuum[50,52] (Figure 1.5). A similar conclusion was reached by Sun and co-workers[53] for Ge(111) surfaces. Unlike Ge(111) surfaces, which only forms a monochloride phase, Ge(100) surfaces can have both monochloride and dichloride species, at each Ge(100) surface.
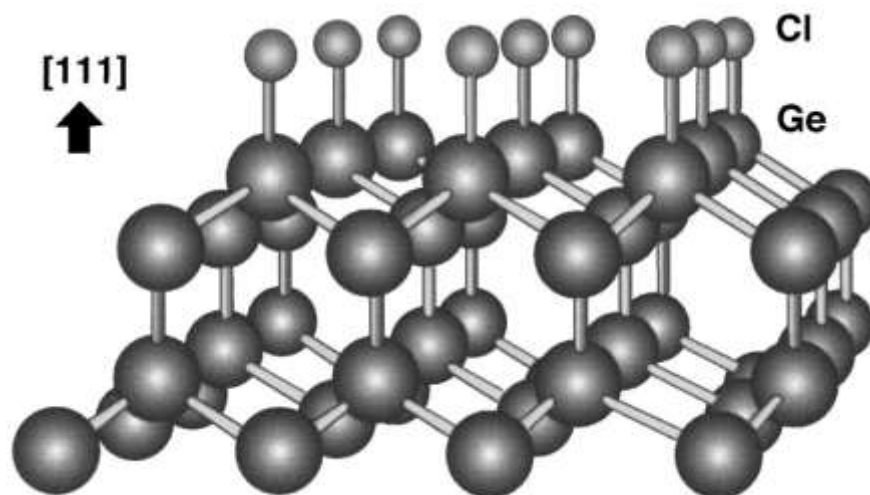
Figure 1.5:   Schematic view of a Cl-terminated Ge(111) surface.
(Lu ZH. *Appl. Phys. Lett*. **1996**, 68:520–22)

1.2.3 Hydride passivation

The production of atomically flat, well ordered, and chemically clean interfaces is crucial to many semiconductor device technologies. The ideal surface passivation layer has each hydrogen atom bonding to a single-surface dangling bond.

On silicon, hydride termination is well researched and provides many advantages, including aqueous stability and limited air stability[54]. There are two main procedures used for hydrogenation of Si surfaces. In the first method, wet chemical etching of Si samples in aqueous HF solutions, hydrogen-terminated Si surfaces of high quality can be created. For example, an atomically flat Si(111) surface can be prepared reproducibly by using standard aqueous HF solutions[55,56,57]. However, Higashi and co-workers[58,59] found that the pH of the HF solution drastically altered the microscopic roughness and the nature of the associated H termination of the surfaces. They observed that basic solutions (pH=9-10) produced ideally smooth H-terminated Si(111) surfaces. In addition, they demonstrated using STM that the Si(111) surfaces prepared at room temperature using NH_4F solution are atomically flat, compared with the atomically rough surfaces made in aqueous HF solution. The wet chemical method encountered more difficulties for Si(001) surfaces[60,61,62,63]. The hydroxide ions in the solution etch the Si surface to form (111) facets. When the (111) microfacets appear on the Si(001) surface during treatment, the surface becomes rough; and the surface is covered mostly with dihydrides making the surface unstable and rough[64].

An alternative preparation method of hydrogen-terminated Si surfaces is in-situ

exposure of the atomically clean Si surfaces to atomic hydrogen in an ultra-high vacuum (UHV) chamber. Hydrogen adsorption kinetics is the same for 2×1 and 7×7-reconstructed Si(111) surfaces[66]. LEED observations revealed that atomic H exposure of the Si(111)- 2×1 reconstructed surface changes surface structure to the 1×1[65-68]. In a molecular dynamics study, Ancilotto and Selloni[69] found that the 1×1 bulk-like structure becomes energetically favored over the 2×1 when starting with an H coverage of 0.3 ML. The resulting 1×1 hydrogen surface was less rough compared to that obtained by hydrogenation of the Si(111)-7×7 surfaces. For room temperature adsorption of atomic hydrogen onto Si(100)- 2×1 surface, adsorption takes place very quickly and linearly with exposure when the coverage is below 1 ML. For higher H atom exposures, adsorption occurs slowly towards a saturation coverage of slightly less than 2.0 ML. LEED observation revealed that 2×1 surface periodicity was observed at about 1 ML hydrogen coverage, but the hydrogen saturated surface displays a 1×1 pattern[70,71]. During the initial stage of adsorption, atomic hydrogen reacts at the Si dangling bonds leading to the formation of the monohydride/- Si(100)-2×1 surface (Figure 1.6(a)). For exposures greater than 1 ML, the H atoms break the Si dimer to form the dihydride/-Si(100)-1×1 surface (Figure 1.6(b)). At the highest exposures, the breaking of Si-Si back bonds takes place to produce a trihydride species. The formation of a well-ordered monohydride Si(100)-2×1 surface is possible with a saturation exposure to atomic hydrogen at 350-400℃[70,72,73,74.] The structure of the monohydride phase is widely accepted to form symmetric Si-Si dimers with two

H atoms saturating the dimer dangling bonds (Figure 1.6(b))[75,76,77]. The monohydride Si(100)-2×1 can also be obtained by thermal decomposition of the dihydride Si(100)-1×1 phase in the 250℃ temperature range[78]. Additionally, another well-defined ordered H/Si(100) surface phase, Si(100)-3×1, is formed upon atomic H adsorption at intermediate temperatures of 110±20℃[70,71,73,74,79-81]. The structure of 3×1 phase is considered to consist of alternating monohydride and dihydride species (Figure 1.6(c)).
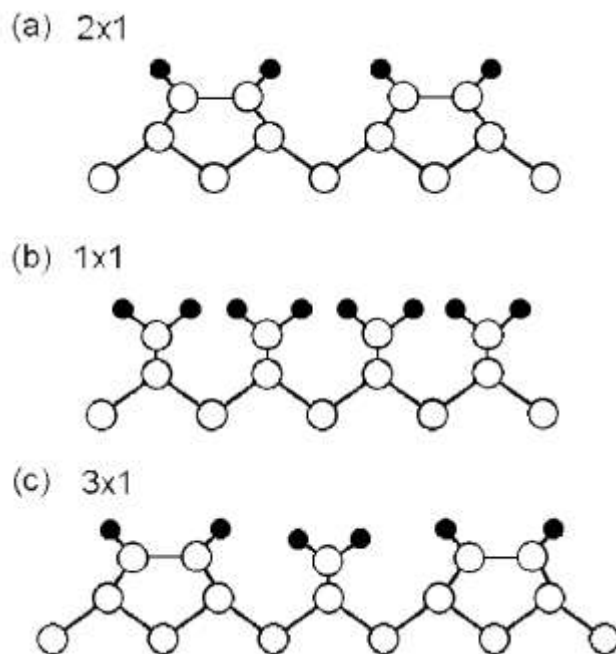
Figure 1.6:   Schematic illustration of the structure of the ordered H/Si(100) surface phased: (a) Si(100)- 2×1 monohydride, (b) Si(100)- 1×1 dihydride, (c) Si(100)- 3×1 monohydride plus dihydride. Solid circles denote H atoms and open circles represent Si atoms.
(K. Oura, V. G. Lifshits, A. A. Saranin, A. V. Zotov, M. Katayama., *Surf. Sci. Rep*. **1999**, 35, 1-69)

Germanium might be expected to be similar to silicon. Hydride-terminated germanium can be obtained in vacuum by adsorption of atomic hydrogen on the

germanium surface. The monohydride Ge(100)-2×1 phase has been well established, which is analogous to the monohydride Si(100)-2×1 phase. However, there is ongoing debate with regard to the formation of a surface dihydride phase. HREELS[78] and STM[82] indicated the presence of a dihydride phase. The dangling bonds of the Ge(100) surface could never be completely removed due to hydrogen adsorption and instability of surface dihydride, which inhibits the large-scale formation of 3×1:H and 1×1:H phases. Shimokawa et al.[83] reported a strong dihydride H_2 TPD peak (β_2), concluding that the dihydride formation on Ge(100) was as efficient as that on Si(100). On the other hand, results of hydrogen desorption studies from Ge(100) vary a lot, from the observation of no dihydride[84, 85, 86] to a clearly distinguishable dihydride desorption state[87]. These mixed results are in contrast to the clear dihydride phase that is formed upon increasing hydrogen exposure on the Si(100)-2×1 surface.

A dilute HF solution is used to produce a hydrogen-terminated surface for both the Ge(100) and Ge(111) surfaces[32]. The nature of the hydride termination has been studied on Ge(100). From the thermodynamic point of view, the Ge-F bond (116 kcal/mol) is more stable than the Ge-H bond (77 kcal/mol). Research shows that kinetics plays a more important role in the hydride-terminated germanium surface[88]. During the etching process, the HF concentration plays a key role in determining the hydrogen coverage. However, in this study a perfect hydrogen terminated Ge(100) surface could not be achieved, even with high HF concentrations. It is reported that the Ge surface is influenced more by the concentration of HF than Si surface[53,89]. This

result appears to be due to the electronegativity difference between Si and F which is greater than that between Ge and F, and Si-F bonds are stronger and shorter than Ge-F bonds (the bond strength: Si-F 553 kJ/mol, Ge-F 485kL/mol; the bond length: Si-F 1.58 Å, Ge-F 1.73 Å)[90]. In addition, the Si-Si back bonds are polarized more, thus making it easier for reaction with HF. Rivillon and Chabal[91] determined by infrared absorption spectroscopy and x-ray photoemission spectroscopy that hydrogen passivated Ge (100) surfaces without oxide were obtained by using HF wet chemical methods, but the etched Ge surfaces were atomically rough, and displaying mostly monohydride and dihydride species. When exposed to ambient air, H-terminated Ge(100) is unstable, exhibiting rapid hydrocarbon contamination, but no immediate oxide growth. The slow rate of oxide regrowth under ambient condition is consistent with Deegan and Hughes[32], who showed that the hydride terminated surface to still be reactive.

1.3 Organic functionalization reactions

The formation of organic monolayers on semiconductor surfaces has recently become an area of intense investigation. One important motivation is the need to control electronic properties by covalently attaching molecules to the semiconductor surface[92]. Another driving motivation is to incorporate organic molecular properties, such as chemical affinity, flexibility, conductivity, and chirality for developing biomedical sensors[93,94]. Organic functionalization has been carried out in both solution and dry vacuum environments. Figure 1.7 shows some of the commonly used

methods for organic monolayer functionalization.

1.3.1 Dry chemical functionalization

As mentioned earlier, Si(100)-2×1 and Ge(100)-2×1 surfaces are characterized by

a surface reconstruction in which adjacent atoms pair together to form dimer bonds

that can be thought of as weak π-bonds. The π bond in the dimer is weaker than a

π-bonds in alkenes (5-10 kcal/mol for Si and 2-8 kcal/mol for Ge)[95]. The presence of

the weak π-bond at the surface also presents the possibility of cycloaddition-like

reaction between Si or Ge dimers and an alkene[1,96-111] (Figure 1.7a and b).
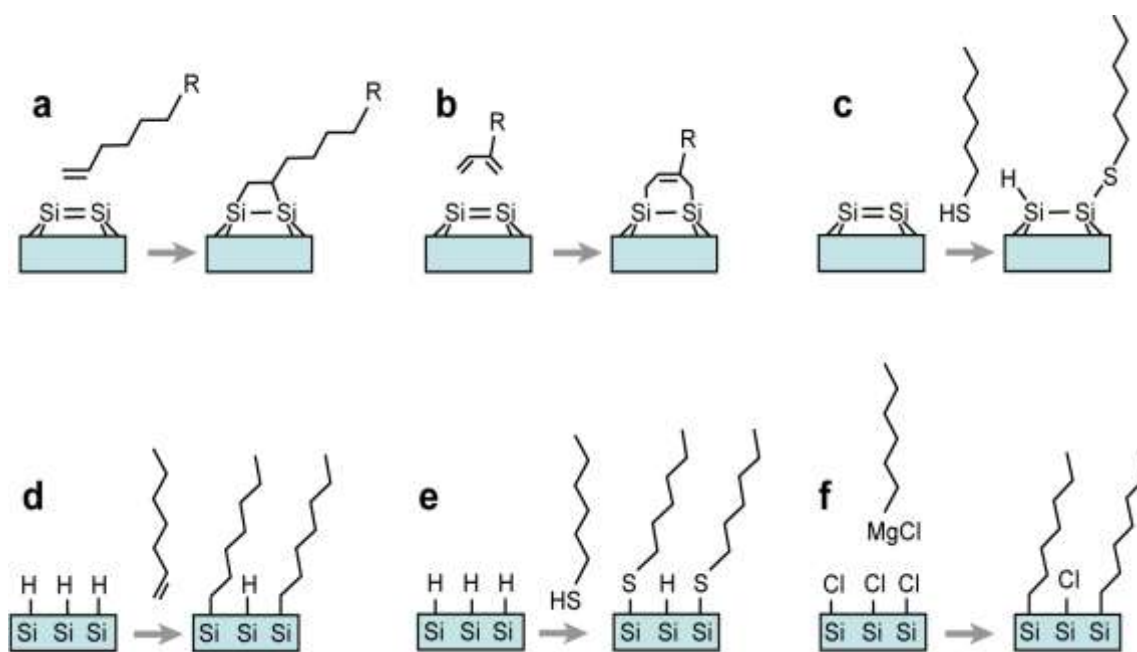
Figure 1.7: Commonly used methods for forming organic monolayers on semiconductor surfaces. Panels *a–c* depict methods used in dry vacuum conditions. Panels *d–f* depict methods used in wet chemical environments on hydrogen-passivated or halogen-passivated surfaces. (Hamers, R. J. *Annu. Rev. Anal. Chem.* **2008**, 1, 707–736)

1.3.1.1 [2+2]/[4+2]Cycloaddition reactions

One mechanism for addition of an unsaturated organic molecule with Si/Ge (100)- 2×1 dimers is a [2+2] cycloaddition reaction, in which two electrons from the C=C π-bond of the unsaturated organic molecule and two electrons from the π-bond of the surface dimer link together, and eventually form a four-member ring at the interface (Figure 1.8 a). This reaction is symmetry forbidden[96]. However, the tilting of the surface dimer breaks the symmetry and allows the reaction to proceed. The resulting covalent bonds between the organic molecule and the underlying Si/Ge surface also implies that the orientation of the underlying dimers is translated into the orientation of the upper organic molecular layer. Hamers and co-workers[116, 117] showed that a fabricated molecular layer on silicon could be achieved by choosing small cyclic molecules that are highly symmetric and relatively rigid.
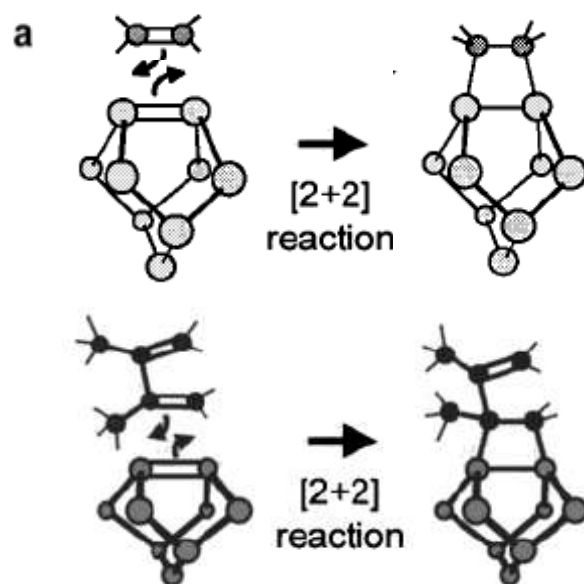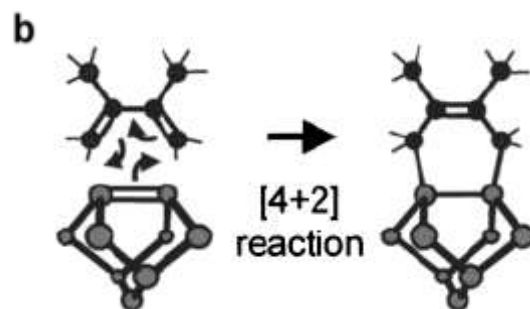
Figure 1.8: Scheme of cycloaddition reaction on Si/Ge surface. (a) [2+2] cycloaddition reaction. (b) [4+2] Diels-Alder Reactions

The reaction of most saturated organic molecules with Si or Ge surfaces involve large thermal activation barriers associated with cleavage of C-C or C-H bonds, but cycloaddition-like reactions of unsaturated organic molecules do not require much energy for bond cleavage[23]. Several studies have shown that the attachment with somewhat complex and organic molecules, such as cyclopentene[96,110,112], 1,3,5,7-cyclooctatetraene[98], 3-pyrroline[99,100], benzene[113] and styrene[114,115] can readily occur on silicon and germanium surfaces.

A second type of cycloaddition-like reaction can take place if there are conjugated double bonds in the reacting organic molecule. It is similar to a "Diels-Alder" reaction in organic chemistry. In this reaction, four electrons from the diene and two electrons of the Si/Ge dimer interact to form a six-member ring at the interface (Figure 1.8 b). In this case, the reactant molecule must contain two conjugated double bonds (a 'conjugated diene'). When complex molecules with conjugated π electron structures interact with Si/Ge dimer, multiple products including [2+2] reaction products and [4+2] reaction products are observed as in the

case of 1,3-dienes[109], 1,3-cyclohexadiene[111], 1,3-butadiene[23] and benzene[113]. These studies showed the challenges in controlling the selective functionalization in order to obtain well-ordered monolayers on the semiconductor surface. For these dienes, there is a competition between [2+2] and [4+2] cycloaddition reactions. The exception seems to be substituted aromatic compounds. An interesting example is styrene, where the substituent group binds to the surface, leaving the aromatic ring intact[118-120].

Because of the similarity between Ge(100)-2×1 and Si(100)- 2×1 surfaces, these same types of cycloaddition reactions also occur at the Ge surfaces. However, important differences between the two surfaces have become evident. Firstly, on Si(100)-2×1, cyclopentene forms a well-ordered monolayer at saturation coverage with about one cyclopentene molecule per Si-Si dimer. In contrast, the coverage on Ge(100)- 2×1 at saturation is approximately two cyclopentene molecules per three germanium dimers[121,122]. Secondly, the reversibility of the adsorption process is different on the two surfaces. On the germanium surface, 1,3-butadiene reversibly desorbs[123], while on the silicon surface, it largely decomposes instead of desorbing[103,104]. Mui et al. concluded that the binding energy of the Diels-Alder product was lower on Ge than on Si owing to the Ge-C bonds were 7-9 kcal/mol weaker than the Si-C bonds[124].

1.3.1.2 Reactions involving functional groups

Some simple functional groups, such as the thio, amino, and hydroxyl groups have labile hydrogen atoms that can be easily removed. Based on this characteristic,

they are able to link to the semiconductor surface through S, N or O atoms (Figure 1.7 c). In the process, a hydrogen atom is transferred to the surface as the S-H, N-H or O-H bond cleaves.

1.3.1.3 Reactions involving dative bond

It is desirable to produce well-ordered monolayers of multifunctional molecules where one reactive group links to the surface and the other functional group is available for further reaction. A novel route that involves dative bonding is being investigated[125-129]. The key to this method is a Lewis acid-base reaction between the N atom in the molecule and the down atom of the dimer on the Si(100) or Ge(100) surface. It is recognized that the dimers of the Si or Ge(100) surfaces have zwitterionic character associated with an "up" dimer atom protruding from the surface and a "down" dimer atom recessed in the surface. The electron density at the up atom of the dimer is higher than that of the down atom, leading to nucleophilic and electrophilic character respectively (Figure 1.1 d). When N-containing organic molecules, for example an amine, approach the Si or Ge (100) dimer, the nitrogen lone pair electrons interact with the electrophilic down atom of a tilted dimers to form a dative bond via a Lewis acid-base reaction (Figure 1.9).
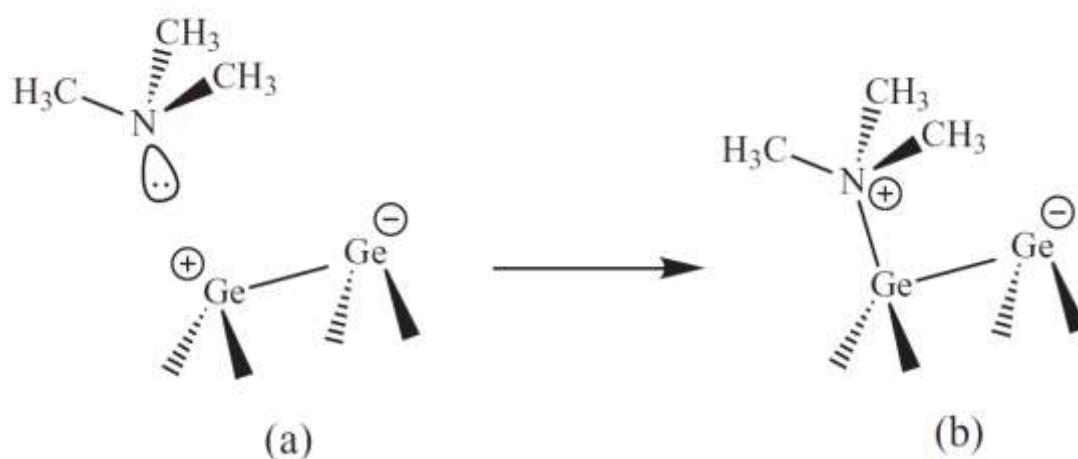
Figure 1.9: Illustration of the surface reaction of trimethylamine with Ge(100)-2×1 leading to the formation of a dative bond.
(Loscutoff W. P.; Bent F. S. *Annu. Rev. Phys. Chem.* **2006**, 57, 467-495.)

Primary and secondary amines undergo N-H dissociation from the dative-bound state. A hydrogen atom is transferred to the neighboring atom in the same dimer (showed in Figure 1.10) as the dative bound state reacts with the surface. However, Mui et al.[130] found that N-H cleavage in methylamines did not occur on germanium surfaces in some cases, due to the larger activation barrier for N-H cleavage on Ge compared with that on Si.
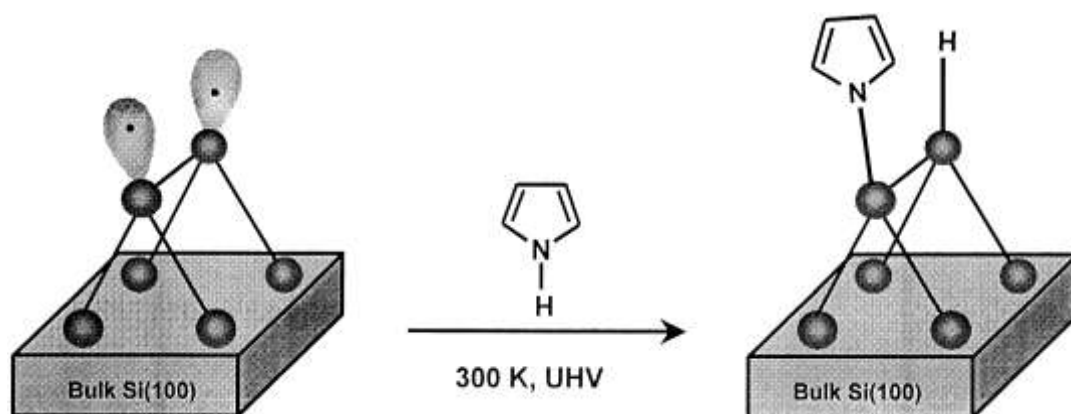
Figure 1.10: A schematic model of dative bonding formation and attachment of the dissociated hydrogen atom to the neighboring atom in the same dimer. (Qiao, M. H.; Cao, Y.; Deng, J. F.; Xu. G. Q. *Chem. Phys. Lett*. **2000**, 325, 508-512.)

1.3.2 Wet chemical functionalization

Organic monolayers on semiconductor surfaces can also be made under wet chemical conditions as shown in Figure 1.7 d-f. Three common methods of wet chemical functionalization have been studied on silicon or germanium surface: (a) hydrosilylation/ hydrogermylation reaction, (b) Grignard reaction on chloride-terminated surfaces, (c) alkanethiol reactions.

1.3.2.1 Hydrosilylation/ Hydrogermylation reaction

Of the wet chemical functionalization methods for semiconductor surface, hydrosilylation/ hydrogermylation is the most extensively studied. Once a hydrogen-terminated surface is obtained, reaction with alkenes or other unsaturated compounds can occur as depicted in Figure 1.7 d. A variety of monolayers have been reported from alkenyl and alkynyl reaction with the hydrogen-terminated Si(100) and Ge(100)

surfaces[54,88]. Similarly, surfaces alkylated by hydrogermylation show enhanced surface stability.

1.3.2.2 Grignard reaction

Surface alkylation by Grignard reagents was conducted beginning with an ordered chloride-terminated Si or Ge(100) surface, prepared by exposure to dilute HCl. Then a Grignard reagent containing an alkyl chain, ranging from ethyl to octadecyl is used to, link to the semiconductor surface[1,131]. The Grignard-alkylated surfaces show increased surface stability, and attached organic monolayers could possibly impart specifically enhanced reactivity.

1.3.2.3 Alkanethiol reactions

Whereas both two kinds of reactions indicated above create a Si or Ge-C bonds during the attachment reaction to the surface, alkanethiol reactions create a Si or Ge-S-C bonds (Figure 1.7 e). But the interface is less stable than the corresponding direct surface alkylation through Si or Ge-C bond formation. Han et al. suggested that the decreased surface stability resulted from the weaker strength of the Ge-S bond compared to the Ge-C bond[132].

1.4 X-ray Photoelectron Spectroscopy Characterization

1.4.1 Background

X-ray Photoelectron Spectroscopy (XPS), also known as Electron Spectroscopy for Chemical Analysis (ESCA) is a widely used technique to investigate the chemical composition of surfaces. The surface to be analyzed is first placed in a vacuum

environment and then irradiated with photons. The atoms on the surface emit electrons (photoelectrons) after direct transfer of energy from the photon to the core-level electron. The process is showed in Fig 1.11. The emitted electrons are then separated according to energy and counted. The energy of the emitted photoelectrons is related to the atomic and molecular environment from which they originated. The number of electrons emitted is related to the concentration of the emitting atom in the sample[133]. XPS is based on Einstein's idea about the photoelectric effect (Figure 1.12), developed around 1905. In the photoelectric effect, electrons are emitted from matter (metals and non-metallic solids, liquids or gases) as a consequence of their absorption of energy from electromagnetic radiation of very short wavelength, such as visible or ultraviolet light[134,135]. It describes the ejection of electrons from a surface when photons were impinged upon it. During the mid 1960's Dr. Siegbahn and his research group developed the XPS technique and finally produced the first commercial monochromatic XPS instrument in 1969. Siegbahn received the Nobel Prize in 1981 for the development of XPS[136].

In simple terms, x-ray photoelectron spectroscopy involves the ionization of bound electrons from a sample and the measurement of the kinetic energy of the electrons. The kinetic energies, for a fixed photon energy, depend mainly on the chemical elements from which the electrons originate and to a lesser extent upon the chemical environments of those elements.
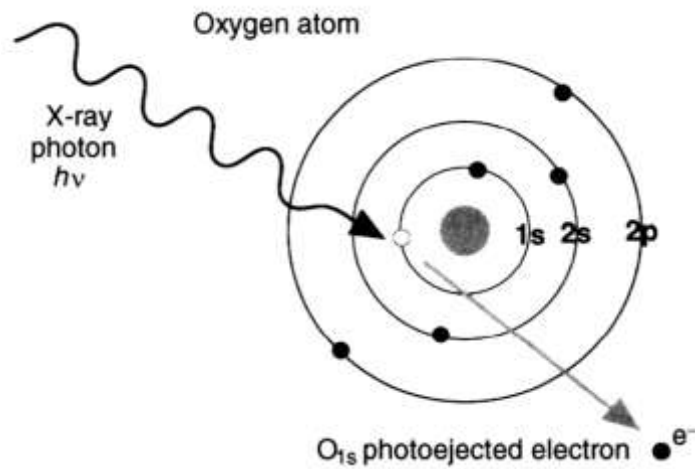
Figure 1.11:   The X-ray photon transfers enough energy to a core-level electron to Cause its ejection from the atom
(Buddy D. Ratner, David G. Castner. Surface Analysis- The Principal Techniques Chapter 3)
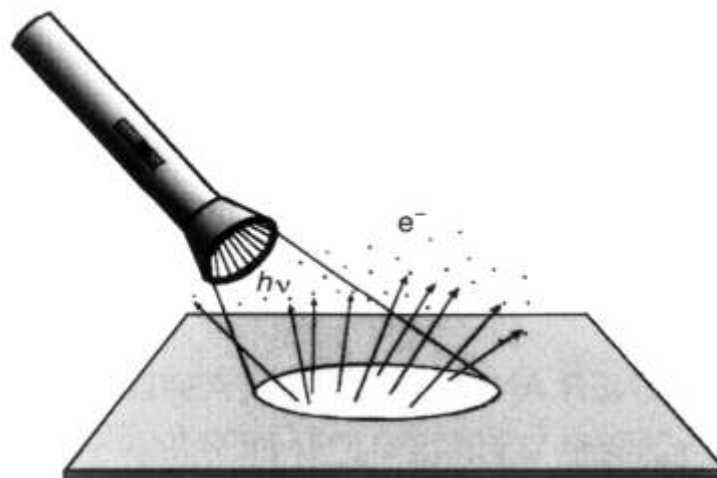
Figure 1.12:   Schematic of the photoelectric effect
(Buddy D. Ratner, David G. Castner. Surface Analysis- The Principal Techniques Chapter 3)

In XPS, the X-ray irradiates the sample surface, hitting the core electrons (e-) of the atoms. The core electrons are close to the nucleus and have binding energies

characteristic of their particular element. An electron near the Fermi level is more delocalized from the nucleus and is moving in different directions. The Fermi level is the highest occupied energy level by an electron in a neutral solid at absolute zero temperature. Electron binding energy (BE) is calculated with respect to the Fermi level. The BE is determined by the attraction of the electrons to the nucleus[137]. An electron, which is negatively charged, is attracted to the nucleus of an atom because of the positive charge. The amount of energy that is required for an electron to be removed from the solid is called the binding energy[138]. If an electron with energy is pulled away from the nucleus, the attraction between the electron and the nucleus decreases and the BE decreases. Eventually, there will be a point when the electron will be free of the nucleus. The ejected photoelectron has kinetic energy:

$$KE=hv\text{-}BE\text{-}\Phi \qquad\qquad (1.1)$$

Where: KE = electron kinetic energy (in eV)

hv =the energy of the X-ray source

BE = binding energy of the electron in the atom

Φ = work function which is the minimum energy required to eject an electron

from highest occupied level into vacuum

But, the atom in an (n-1) electron state sometimes can reorganize by dropping an electron from a higher energy level to a vacant core hole. Subsequently, the atom can get rid of the excess energy by ejecting an electron from a higher energy level. This ejected electron is referred to as an Auger electron. The difference between

photoelectron and Auger electron ejected from irradiated atom is showed below as Figure 1.13.
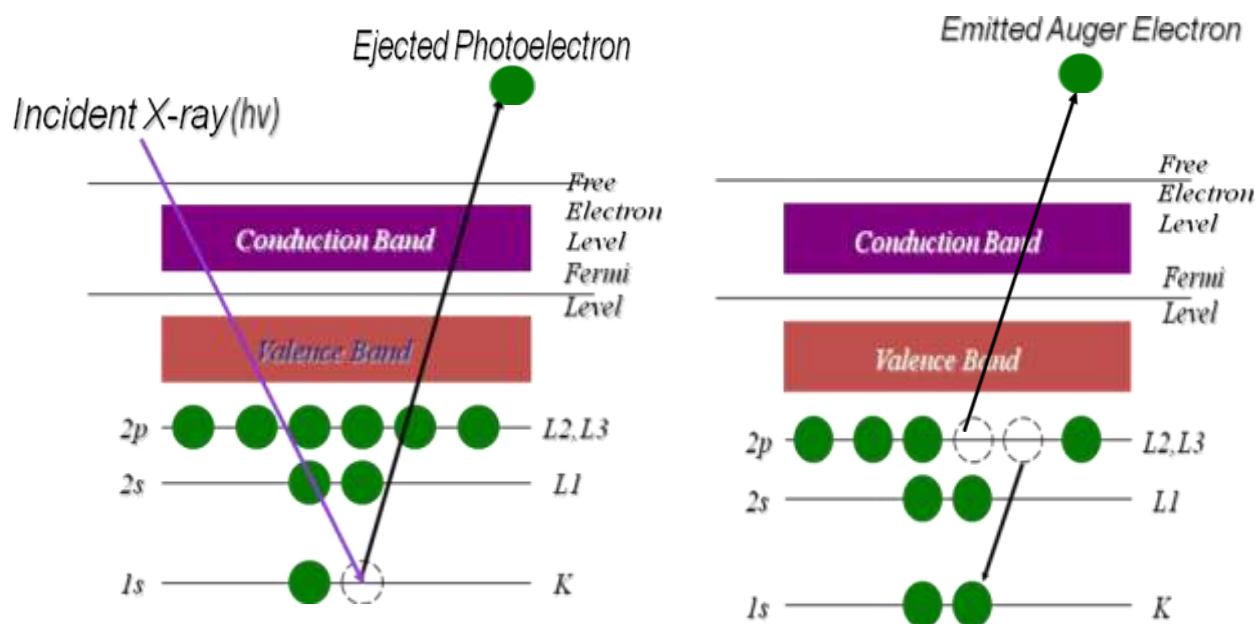
Figure 1.13: The Photoelectric Process (on the left).
The process of emitted Auger electron (on the right)

1.4.2 Quantitative analysis by XPS

It is meaningful to know the concentration of some species derived from reactants which could eliminate many possible reaction paths and stoichiometries. In most cases, absolute concentration can not be determined, but we can draw some conclusions about ratios of elemental concentrations. The complete ESCA spectrum of a material contains peaks that can be associated with the various elements (except H and He) present in the outer 10 nm of that material. The area under these peaks is related to the amount of each element present. Therefore, by measuring the peak areas and correcting them for the appropriate instrumental factors, the percentage of each

element detected can be determined.

In a general sense, the following factors must be considered to give a relation between the measured intensity, I, and the number density of a certain kind of atom, n:

$$I = n \times F \times \theta \times \sigma \times A \times \lambda \times T \qquad (1.2)$$

Where: F = x-ray flux;

θ = angular factor;

σ = photoionization cross section;

A = area sampled;

λ = electron mean free path;

T = detection efficiency

The most common approach is to compare one sample with another one under identical, or at least reproducible, conditions using two or more XPS lines per sample. In this way, some factors cancel and the ratio of the measured intensity, I, and the number density of atom, n, is obtained:

$$\frac{n_A}{n_B} = \left(\frac{I_A}{I_B}\right) \times \left(\frac{S_B}{S_A}\right) \qquad (1.3)$$

Where: S is an instrumental sensitivity factor that includes all of the variables listed above;

Assuming that the measurements are made under identical conditions of flux, angular, and area conditions and detection efficiencies, S_A reduces to a product of the cross section(σ) and the mean free path(λ):

$$S_A = \sigma_A \times \lambda_A \qquad (1.4)$$

And the mean free path for electrons with kinetic energies above 100 eV

increases roughly as $(KE)^{0.75}$. So equation 1.3 can be rewritten:

$$\frac{n_A}{n_B} = \left(\frac{I_A}{I_B}\right) \times \left(\frac{S_B}{S_A}\right) \times \left(\frac{KE_B}{KE_A}\right)^{0.75} \qquad (1.5)$$

Equation 1.5 can then be used to determine the atomic ratio of elements to help

determine the composition of the sample's surface.

1.5 References

1. Hamers, R. J. *Annu. Rev. Anal. Chem.* **2008**, 1, 707–736.

2. Hochberg, L. R.; Serruya, M. D.; Friehs, G. M.; Mukand, J. A.; Saleh, M.; Caplan, A. H.; Branner, A.; Chen, D.; Penn, R. D.; Donoghue, J. P. *Nature* **2006**, 442, 164–171.

3. He, Y.; Su, Y. Y.; Yang, X. B.; Kang, Z. H.; Xu, T. T.; Zhang, R. Q.; Fan, C. H.; Lee, S. T. *J. Am. Chem. Soc.* **2009**, 131, 4434–4438.

4. Erogbogbo, F.; Yong, K. T.; Roy, I.; Xu, G. X.; Prasad, P. N.; Swihart, M. T. *ACS Nano* **2008**, 2, 873–878.

5. Martinez, J. A.; Misra, N.; Wang, Y. M.; Stroeve, P.; Grigoropoulos, C. P.; Noy, A. *Nano Lett*. **2009**, 9, 1121–1126.

6. Qu, Y. Q.; Liao, L.; Li, Y. J.; Zhang, H.; Huang, Y.; Duan, X. F. *Nano Lett*. **2009**, 9, 4539–4543.

7. Kilian, K. A.; Bocking, T.; Gaus, K.; Gal, M.; Gooding, J. J. *Biomaterials* **2007**, 28, 3055–3062.

8. Singamaneni, S.; LeMieux, M. C.; Lang, H. P.; Gerber, C.; Lam, Y.; Zauscher, S.; Datskos, P. G.; Lavrik, N. V.; Jiang, H.; Naik, R. R.; Bunning, T. J.; Tsukruk, V. V. *AdV. Mater*. **2008**, 20, 653–680.

9. Yam, C. M.; Xiao, Z. D.; Gu, J. H.; Boutet, S.; Cai, C. Z. *J. Am. Chem. Soc*. **2003**, 125, 7498–7499.

10. Jonkheijm, P.; Weinrich, D.; Schroder, H.; Niemeyer, C. M.; Waldmann, H. *Angew. Chem., Int. Ed*. **2008**, 47, 9618–9647.

11. Nijdam, A. J.; Cheng, M. M. C.; Geho, D. H.; Fedele, R.; Herrmann, P.; Killian, K.; Espina, V.; Petricoin, E. F.; Liotta, L. A.; Ferrari, M. *Biomaterials* **2007**, 28, 550–558.

12. Stern, E.; Vacic, A.; Rajan, N. K.; Criscione, J. M.; Park, J.; Ilic, B. R.; Mooney, D. J.; Reed, M. A.; Fahmy, T. M. *Nat. Nanotechnol.* **2010**, 5, 138–142.

13. Fromherz, P. *Solid-State Electron.* **2008**, 52, 1364–1373.

14. Meuris, M. *EE Time.* **2003**, August 22.

15. Loscutoff, W. P.; Bent F. S. *Annu. Rev. Phys. Chem.* **2006**, 57, 467-495.

16. Zandvliet, H. J. W. *Phys. Rep.* **2003**, 388, 1-40.

17. Appelbaum, J. A.; Baraff, G. A.; Hamann, D. R. *Phys. Rev.* 1**976**, B 14, 588-601.

18. Needels, M.; Payne, M. C.; Joannopoulos, J. D. *Phys. Rev.* **1988**, B 38, 5543-5546.

19. Jing, Z.; Whitten, R.L. *Phys. Rev.***1994**, B 50, 2598.

20. Hukka, T. I. ; Pakkanen, T. A.; Evelyn, M. P. D. *J. Phys. Chem.* **1994**, 98, 12420.

21. Weiner, B.; Skokov, S.; Frenklach*, M. J. Chem. Phys.* **1995**, 105, 5486.

22. Kress, C.; Fiedler, M.; Schmidt, W. G.; Bechstedt, F. *Phys. Rev.***1994**, *B* 50, 17697.

23. Hamers, R. J.; Coulter, S. K.; Ellison, M. D.; Hovis, J. S.; Padowitz, D. F.; Schwartz, M. P.; Greenlief, C. M.; Russell Jr., J. N. *Acc. Chem. Res.* **2000**, 33, 617-624.

24. Mui, C.; Han, J. H.; Wang, G. T.; Musgrave, C.B. *J. Phys. Chem*. **2003**. B 107: 12256-67.

25. Ludeke, R.; Koma, A. *Phys. Rev. Lett*. **1975**, 34 (18), 1170-1173.

26. Hovis, J. S.; Hamer, R. J.; Greenlief, C. M. *Surf. Sci*. **1999**, 440, L815-L819.

27. Hollinger, G.; Himpsel, F. J. *J. Vac. Sci. Technol*. **1982**, A 1:640–45.

28. Hollinger, G; Himpsel, F. J. *Appl. Phys. Lett*. **1984**, 44:93–95.

29. Prabhakaran, K.; Ogino, T. *Surf. Sci*. **1995**, 325, 263-271.

30. Chan, L. H.; Altman, E. I.; Liang, Y. *J. Vac. Sci. Technol*. **2001**, A 19:976–81.

31. Cho, J. W.; Nemanich, R. J. *Phys. Rev. B, Condens. Matter* **1992**, 46:12421–26.

32. Deegan, T.; Hughes, G. *Appl. Surf. Sci*. **1998**. 123/124:66–70.

33. Kim, J.; Saraswat, K.; Nishi, Y. *ECS Trans.* **2005**, 1(3):214–19.

34. Ma, Q.; Moldovan, N.; Mancini, D. C.; Rosenberg, R. A. *Appl. Phys. Lett.* **2002**, 81:1741–43.

35. Okumura, H.; Akane, T.; Matsumoto, S. *Appl. Surf. Sci*. **1998**, 125:125–28.

36. Prabhakaran, K.; Ogino, T.; Hull, R.; Bean, J. C.; Peticolas, L. J. *Surf. Sci.* **1994**, 316:L1031–33.

37. Zhang, X. J.; Xue, G.; Agarwal, A.; Tsu, R.; Hasan, M. A. et al. *J. Vac. Sci. Technol.* **1993**, A 11:2553–61.

38. Park, K.; Lee, Y.; Lee, J.; Lim, S. *Appl. Surf. Sci.* **2008**, 254, 4828-4832.

39. Weser, T.; Bogen, A.; Konrad, B.; Schnell, R. D.; Schug, C. A. et al. **1988**. Surf. Sci. 201:245–256.

40. Weser, T.; Bogen, A.; Konrad, B.; Schnell, R. D.; Schug, C. A.; Steinmann, W. *Phys. Rev. B, Condens. Matter* **1987**, 35:8184–8188.

41. Kaxiras, E. *Phys. Rev.* **1991**, *B*43, 6824.

42. Roche, J.; Ryan, P.; Hughes, G. *Surf. Sci.* **2000**, 465: 115-119.

43. Papageorgopoulos, A.; Corner, A.; Kamarators, M.; Papageorgopoulos, C. A. *Phys. Rev.* **1997**, B 55: 4435.

44. Papageorgopoulos, A. *Solid State Commun.* **1997**, 101, 383.

45. Anderson, G. W.; Hanf, M. C.; Norton, P. R.; Lu, Z. H.; Graham, M. J. *Appl. Phys .Lett.* **1995**, 66:1123–25.

46. Lyman, P. F.; Sakata, O.; Marasco, D. L.; Lee, T. L.; Breneman, K. D. et al. *Surf. Sci.* **2000**, 462:L594–98.

47. Tromp, R. M.; Hamers, R. J.; Demuth, J. E. *Phys. Rev. Lett.* **1985**, 55, 1303.

48. Cullen, G. W.; Amick, J. A.; Gerlich, D. *J. Electrochem. Soc.* **1962**, 109:124–27.

49. Schnell, R. D.; Himpsel, F. J.; Bogen, A.; Rieger, D.; Steinmann, W. *Phys. Rev. B, Condens. Matter* **1985**, 32:8052–56.

50. Lu, Z. H. *Appl. Phys. Lett*. **1996**, 68:520–22.

51. *CRC Handbook of Chemistry and Physics*, edited by R. C. Weast (CRC, Boca Raton, FL, **1985**)

52. Citrin, P. H.; Rowe, J. E.; Eisenberger, P. *Phys. Rev. B, Condens. Matter* **1983**, 28:2299–301.

53. Sun, S.; Sun, Y.; Liu, Z.; Lee, D.; Peterson, S.; Pianetta, P. *Appl. Phys. Lett.,* 88, (021903) **2006**.

54. Buriak, J. M. *Chem. Rev.* **2002**, 102:1271–308.

55. Higashi, G. S.; Chabal, Y. J.; Trucks, G. W.; Raghavachari, K. *Appl. Phys. Lett*. **1990**, 56, 656.

56. Watanabe, S.; Nakayama, N.; Ito, T. *Appl. Phys. Lett*. **1991**, 59, 1458.

57. Tokumoto, H.; Morita, Y.; Miki, K. Mater. Res. Soc. *Symp. Proc*. **1992**, 259, 409.

58. Higashi, G. S.; Becker, R. S.; Chabal, Y. J.; Becker, A. J. *Appl. Phys. Lett.* **1991**, 58:1656–58.

59. Higashi, G. S.; Chabal, Y. J.; Trucks, G. W.; Raghavachari, K. *Appl. Phys. Lett.* **1990**, 56:656–58.

60. Chabal, Y. J. *Mater. Res. Soc. Symp. Proc*. **1992**, 259, 349.

61. Morita, Y.; Tokumoto, H. *Mater. Res. Soc. Symp. Proc*. **1994**, 318, 293.

62. Yau, S. L.; Kaji, K.; Itaya, K. *Appl. Phys. Lett*. **1995**, 66, 766

63. Morita, Y.; Tokumoto, H. *Appl. Phys. Lett*. **1995**, 67 (18).

64. Northrup, J. E. *Phys. Rev*. **1991**, *B* 44, 1419

65. Ibach, H.; Rowe, J.E. *Surf. Sci*. **1974**, 43, 481.

66. Schulze, G.; Henzler, M. *Surf. Sci*. **1983**, 124, 336.

67. Akremi, A.; Lacharme, J. P.; Sebenne, C. A. *Surf. Sci*. **1997**, 377/379, 192.

68. Froitzheim, H.; Kohler, U.; Lammering, H. *Surf. Sci*. **1985**, 149, 537.

69. Ancilotto, F.; Selloni, A. *Phys. Rev. Lett*. **1992**, 68, 2640.

70. Oura, K.; Yamane, J.; Umezawa, K.; Naitoh, M.; Shoji, F.; Hanawa, T. *Phys. Rev.* **1990**, *B* 41, 1200.

71. Chabal, Y. J.; Raghavachari, K. *Phys. Rev. Lett*. **1985**, 54, 1055.

72. Schaefer, J. A.; Stucki, F.; Anderson, J. A.; Lapeyre, G. J.; Gopel, W. *Surf. Sci*. **1984**, 140, 207.

73. Boland, J. J. *Phys. Rev. Lett*. **1990**, 65, 3325.

74. Boland, J. J. *Surf. Sci*. **1992**, 261, 17.

75. Shoji, F.; Kashihara, K.; Sumitomo, K.; Oura, K. *Surf. Sci.* **1991**, 242, 422.

76. Shoji, F.; Kashihara, K.; Oura, K. *Surf. Sci.* **1993**, 280, L247.

77. Wang, Y.; Shi, M.; Rabalais, J. W. *Phys. Rev.* **1993**, *B* 48, 1678.

78. Papagno, L.; Shen, X. Y.; Anderson, J.; Spagnolo, G. S.; Lapeyre, G. J. *Phys. Rev. B,* **1986**, 34:7188–91.

79. Cheng, C. C.; YatesJr. J. T. *Phys. Rev.* **1991**, *B* 43, 4041.

80. Jiang, D. T.; Anderson, G. W.; Griffiths, K.; Sham, T. K.; Norton, P. P. *Phys. Rev.* **1993**, *B* 48, 4952.

81. Qin, X. P.; Norton, P. R. *Phys. Rev.* **1996**, *B* 53, 11100.

82. Maeng, J. Y.; Lee, J. Y.; Cho, Y. E.; Kim, S. *Appl. Phys. Lett.* **2002**, 81, 3555.

83. Shimokawa, S.; Namiki, A.; Gamo, M. N.; Ando, T. *J. Chem. Phys.* **2000**, 113, 6916

84. Surney, L.; Tikhov, M. *Surf. Sci.* **1984**, 138, 40

85. Chabal, Y. J. *Surf. Sci.* **1986**, 168, 594

86. Lewis, L. B.; Segall, J.; Janda, K. C. *J. Chem. Phys.* **1995**, 102:7222–28.

87. Shimokawa, S.; Namiki, A.; Gamo, M. N.; Ando, T. *J. Chem. Phys.* **2000**, 113:6916–25.

88. Choi, K.; Buriak, J. M. *Langmuir* **2000**, 16:7737–41.

89. Park, K.; Lee, Y.; Lim, S. *Appl. Surf. Sci*. **2008**, 254, 1842-1846.

90. *CRC Handbook of Chemistry and Physics,* 84th edition, edited by David R. Lide, CRC Press (**2003-2004**).

91. Rivillon, S.; Chabal, Y. *Appl. Phys. Lett*. **2005**, 87, 253101

92. Haran, A.; Waldeck, D. H.; Naaman, R.; Moons, E.; Cahen, D. *Science* **1994**, 263, 948-950.

93. Tao, F.; Xu, G. Q. *Acc. Chem. Res* **2004**, 37, 882-893.

94. Yates, J. T. *Science* **1998**, 279, 335-336.

95. Filler, M. A.; Bent, S. F. *Prog. Surf. Sci.* **2003**, 73:1–56.

96. Hamers, R. J.; Hovis, J. S.; Lee, S.; Liu, H.; Shan, J. *J. Phys. Chem.* **1997**, *B* 101, 1489.

97. Jolly, F.; Bournel, F.; Rochet, F.; Dufour, G. *Phys. Rev.B* **1999**, 60, 2930.

98. Hovis, J. S.; Hamers, R. J *J. Chem. Phys.* **1998**, *B* 102, 687.

99. Hovis, J.S.; Lee, S.; Liu, H.; Hamers, R.J. *J. Vac. Sci. Tech.* **1997**, *B* 15, 1153.

100. Liu, H.; Hamers, R.J. *Surf. Sci.* **1997**, 416, 354.

101. Wang, G. T.; Mui, C.; Musgrave, C. B.; Bent, S. F. *J. Phys. Chem.* **1999**, *B* 103, 6803.

102. Konecny, R.; Doren, D. J. *J. Am. Chem. Soc*. **1997**, 119, 11098.

103. Teplyakov, A.V.; Kong, M. J.; Bent, S.F. *J. Am. Chem. Soc*. **1997**, 119, 11100.

104. Teplyakov, A.V.; Kong, M. J.; Bent, S. F. *J. Chem. Phys*. **1998**, 108, 4599.

105. Liu, H.; Hamers, R. J. *J. Am. Chem. Soc.* **1997**, 119, 7593.

106. Borovsky, B.; Krueger, M.; Ganz, E. *Phys. Rev.* **1998**, *B* 57, R4269.

107. Gokhale, S.; Trischberger, P.; Menzel, D.; Widdra, W.; Droge, H.; Steiuruck, H. P.; Birkenheuer, U.; Getdeutsch, U.; Rosch, N. *J. Chem. Phys*. **1998**, 108, 5554.

108. Kong, M. J.; Teplyakov, A.V; Lyubovitsky, J. G.; Bent, S. F. *Surf. Sci*. **1998**, 411, 286.

109. Hovis, J. S.; Lui, H.; Hamers, R. J. *J. Chem. Phys*. **1998**, *B* 102, 6873.

110. Lee, S. W.; Hovis, J. S.; Coulter, S. K.; Hamers, R. J.; Greenlief, C.M. *Surf. Sci.* **2000**, 462, 6.

111. Lee, S. W.; Nelen, L. N.; Ihm, M.; Scoggins, T.; Greenlief, C.M. *Surf. Sci.* **1998**, 410, L773.

112. Cho, J. H.; Kleinman, L. *Phys. Rev. B, Condens. Matter* **2003**, 67:115314.

113. Fink, A.; Menzel, D.;Widdra, W. *J. Phys.Chem.* **2001**, *B* 105:3828–37.

114. Hwang, Y. J.; Kim, A.; Hwang, E. Y.; Kim, S. *J. Am. Chem. Soc.* **2005**, 127:5016–17.

115. Zhang, Y. P.; Yang, L.; Lai, Y. H.; Xu, G. Q.; Wang, X. S. *Appl. Phys. Lett.* **2004**, 84:401–3.

116. Hovis, J. S.; Hamers, R. J. *J. Phys Chem.* **1997**, *B* 101, 9581.

117. Padowitz, D. F., Hamers, R. J. *J. Phys. Chem.* **1998**, *B* 102:8541–45.

118. Qu, Y. Q.; Han, K. L. *J. Phys. Chem.* **2004**, *B* 108:8305–10.

119. Tao, F.; Wang, Z. H.; Chen, X. F.; Xu, G. Q. *Phys. Rev.* **2002**, *B* 65:115311.

120. Takeuchi, N.; Selloni, A. *J. Phys. Chem.* **2005**, *B* 109:11967–72.

121. Hamers, R. J.; Hovis, J. S.; Greenlief, C. M.; Padowitz, D. F. *Jpn. J. Appl. Phys. Suppl.* **1999**, 38:3879–87.

122. Hovis, J. S.; Liu, H.; Hamers, R. J. *Surf. Sci.* **1998**, 404:1–7.

123. Teplyakov, A.V.; Lal, P.; Noah, Y. A.; Bent, S. F. *J. Am. Chem. Soc.* **1998**, 120:7377–78.

124. Mui, C.; Bent, S. F.; Musgrave, C. B. *J. Phys. Chem.* **2000**, *A* 104:2457–62.

125. Cho, Y. E.; Maeng, J. Y.; Kim, S. Hong, S. Y. *J. Am. Chem. Soc.* **2003**, 125:7514–15.

126. Qiao, M. H.; Cao, Y.; Deng, J. F.; Xu. G. Q. *Chem. Phys. Lett*. **2000**, *325*, 508-512.

127. Seino, K.; Schmidt, W. G.; Furthmu ̈ller, J.; Bechstedt, F. *Phys. Rev. B* **2002**, *66*, 235323-235328.

128. Cao, X.; Coulter, S. K.; Ellison, M. D.; Liu, H.; Liu, J.; Hamers, R. J. *J. Phys. Chem. B* **2001**, *105*, 3759-3768.

129. Lopinski, G. P.; Fortier, T. M.; Moffatt, D. J.; Wolkow, R. A. *J. Vac. Sci. Technol. A* **1998**, *16*, 1037-1042.

130. Mui, C.; Han, J. H.; Wang, G. T.; Musgrave, C. B.; Bent, S. F. *J. Am. Chem. Soc.* **2002**, 124:4027–38.

131. He, J. L.; Lu, Z. H.; Mitchell, S. A.; Wayner, D. D. M. *J. Am. Chem. Soc.* **1998**, 120:2660–61.

132. Han, S. M.; Ashurst, W. R.; Carraro, C.; Maboudian, R. *J. Am. Chem. Soc.* **2001**, 123:2422–25.

133. Ratner, B. D.; Castner, D. G. *Electron Spectroscopy for Chemical Analysis. Chapter 3*

134. Serway, R. A. *Physics for Scientists & Engineers (3rd ed.)*.Saunders. **1990**, pp. 1150

135. Sears, F. W., Zemansky, M. W.; Young, H. D. *University Physics*, Sixth Edition, Addison-Wesley, **1983**, pp. 843-844.

136. Electron Spectroscopy for Atoms, *Molecules and Condensed Matter*, Nobel Lecture,   December 8, **1981**

137. Cardona, M.; Ley, L.; Eds., *Photoemission in Solids I: General Principles,* Springer-Verlag, **1978**.

138. Fuggle, J. C.; Mårtensson, N. *J. Electron Spectrosc*. Relat. Phenom. **1980**, 21, 275

Chapter 2: Experimental Section

2.1 Synthesis of t-butyloxycarbonyl (t-BoC)-protected 11-amino-1-undecene

2.1.1 Material

All chemicals were reagent grade or better and used as received: 1-amino-10-undecene (GFS Chemical, 97%), trifluoroacetic acid (TFA) (Sigma Aldrich, 99% ACS Certified), di-tert-butyl dicarbonate (Aldrich, 99% ACS Certified), methylene chloride (Fisher, ACS Certified), ethyl acetate (Fisher, ACS Certified), hexane (Fisher, ACS Certified), methanol (Fisher, ACS Certified), chloroform (Fisher, ACS Certified), sodium bicarbonate (Fisher, ACS Certified), sodium chloride (Fisher, ACS Certified), magnesium sulfate (Fisher, ACS Certified).

2.1.2 Organic synthesis

t-butyloxycarbonyl (t-BoC)-protected 11-amino-1-undecene was synthesized as follows (Figure 2.1). About 5 g of 1-amino-10-undecene was dissolved into 60 mL of
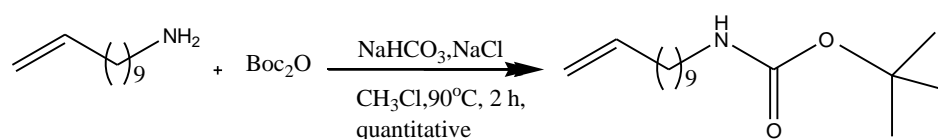

Figure 2.1: Synthesis of t-butyloxycarbonyl (t-BoC)-protected 11-amino-1-undecene.

chloroform, which was added to a solution of 3 g of $NaHCO_3$ in 50 mL of water. 6.45 g of sodium chloride was added along with 7.18 g of di-tert-butyl dicarbonate that

was dissolved in a few milliliters of chloroform[1,2]. The mixture was added to a 250mL Ace round-bottom pressure flask and immersed in a 90 $^{\circ}$C oil bath for 2 hours. After reaction, the collected organic product was extracted twice with 50 mL of diethyl ether. The organic extracts were dried over magnesium sulfate, filtered, and diethyl ether was removed by rotary evaporation.

Although this one-step reaction occurs readily and has high product yield, silicon column chromatography was used to separate the final product in order to purify the t-BOC- protected 1-amino-1-undecene as much as possible. A mixture of 25% ethyl acetate and 75% hexane, by volume, was used as mobile phase solution in the purification step. Finally, vacuum distillation was used to remove any residual water and volatile contaminants.

2.1.3 Characterization with NMR and Mass Spectroscopy

Synthesized t-butyloxycarbonyl (t-BoC)-protected 11-amino-1-undecene was observed in ESI-MS as shown in Figure 2.2. The purity of the compound was also verified by NMR (Figure 2.3).

The biggest peak in the mass spectrum at 214 represents the mass of the protonated ionized fragment of the mother molecule ($C_{11}H_{21}NHCO_2H+H$). The desired mass of the protonated molecule 270 also showed up.
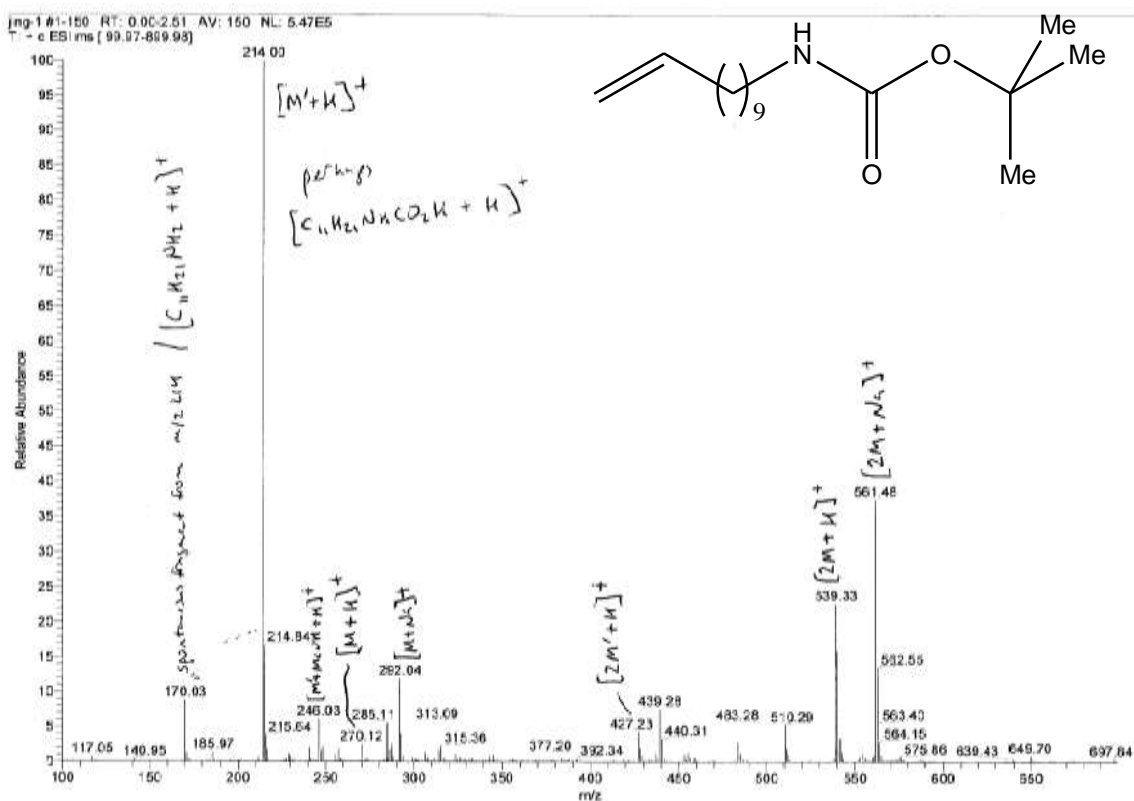
Figure 2.2: ESI-Mass spectrum of synthesized t-butyloxycarbonyl (t-BoC)-protected
11-amino-1-undecene.

Since hydrogens on sp^2 hybridized carbons usually appear between δ6 and δ4.5, the hydrogens with chemical shifts at δ5.81, 4.99, 4.93 should be the hydrogens of the vinyl group. The coupling constants between hydrogens with trans-relationship are bigger than those with cis-relationship. Thus, hydrogen b is distinguished from hydrogen c, based on their coupling constants. The wide peak at δ4.31 should be the hydrogen on the nitrogen atom.
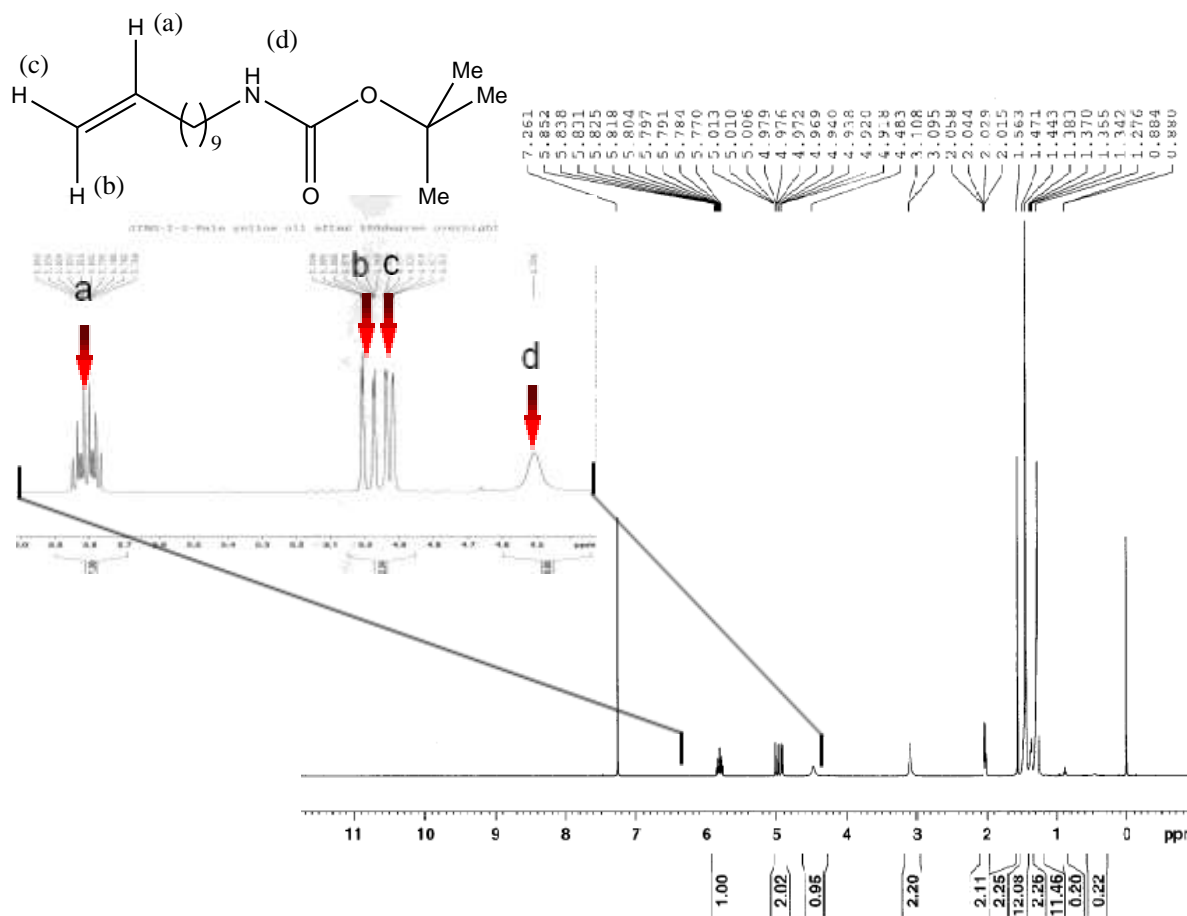
Figure 2.3: NMR spectrum of synthesized t-butyloxycarbonyl (t-BoC)-protected 11-amino-1-undecene.

2.2 Surface studies

2.2.1 H-terminated Si (100) preparation

2.2.1.1 Material and solution preparation

All chemicals were reagent grade or better and used as received: hydrogen peroxide (Fisher, 30% ACS Certified), ammonium hydroxide (Fisher, 14.8N ACS Certified), hydrochloric acid (Fisher, 12.1N ACS Certified), hydrofluoric acid (Fluka, 47%-51% ACS Certified), milli-Q water (18 MΩ), calcium carbonate (Fisher, ACS

Certified). The silicon substrates were cleaved from 3" single-sided polished Si (100) wafers (Virginia Semiconductor, P-doped, 0.035-0.060 Ωcm).

Solution 1 (S1) was prepared from a mixture of 4:1:1 milli-Q water, hydrogen peroxide, and ammonium hydroxide, by volume. Solution 2 (S2) was a mixture of 4:1:1 milli-Q water, hydrogen peroxide, and hydrochloric acid, by volume.

2.2.1.2 H-terminated substrate preparation[1,3,4]

The hydrogen-terminated Si(100) surface was prepared as follows. Two clean 250 mL Teflon beakers were filled 90 mL of S1. Both beakers containing S1 were heated to 80 °C in a water bath. Nitrogen gas was bubbled through each solution for at least 30 minutes. The beakers are removed from the bath, S1 is removed, the beakers are rinsed several times with milli-Q water. The silicon sample is gently blown with nitrogen gas and rinsed with milli-Q water. The sample is then placed in a Teflon beaker that is filled with S1. The beaker containing S1 and the sample are placed into the 80 °C water bath for 10 minutes. The beaker is removed from the water bath and the silicon sample is rinsed several times with milli-Q water. Step three is to add hydrofluoric acid to the Teflon beaker and immerse the silicon wafer for about 2 minutes. The Si sample is removed and rinsed several times with milli-Q water. The fourth step is to transfer the silicon wafer to a Teflon beaker containing enough S2 to completely immerse the sample. Put the beaker into the 80 °C water bath for 10 minutes. Remove the beaker from the water bath, and rinse the silicon wafer several times with milli-Q water. The final step is to etch the silicon wafer and create the

hydrogen-terminated surface. Sufficient 48% concentrated hydrofluoric acid is added to the beaker to completely immerse the silicon sample and the sample is placed in the solution for 1 minute. Remove the sample; rinse it several times with milli-Q water followed by blowing it dry with a steam of dry nitrogen. Because H-terminated Si surfaces will oxidize slowly at atmospheric pressure, they were used as soon as possible after preparation and kept under a nitrogen atmosphere.

2.2.2 H-terminated Ge (100) preparation

2.2.2.1 Material and solution preparation

All chemicals were reagent grade or better and used as received: hydrogen peroxide (Fisher, 30% ACS Certified), ammonium hydroxide (Fisher, 14.8N ACS Certified), hydrochloric acid (Fisher, 12.1N ACS Certified), hydrofluoric acid (Fluka, 47%-51% ACS Certified), milli-Q water (18 MΩ), calcium carbonate (Fisher, ACS Certified), methanol (Fisher, HPLC grade ACS Certified). The germanium substrates used in this work were cut into 0.8×1 cm long strips from p-type Ge (100) wafers purchased from Wafer World (0.10-0.39 Ωcm, resistivity, single-sided polished).

Solution 3 (S3) is a 1:4 mixture of hydrochloric acid and milli-Q water, by volume. Solution 4 (S4) is a mixture of 1:10 hydrogen peroxide and milli-Q water, by volume. Solution 5 (S5) was prepared as a 1:2:20 mixture of ammonium hydroxide, hydrogen peroxide, and milli-Q water, by volume. Concentrated hydrofluoric acid was diluted to 0.5% by using milli-Q water.

2.2.2.2 H-terminated substrate preparation[5,6]

The Ge sample was initially degreased by soaking in HPLC grade methanol. Its oxide layer was stripped by dipping in S3 for 30 seconds and reoxidized by dipping in S4 for 60 seconds. The process of stripping the oxide layer and reforming the oxide layer was repeated three times. After each cycle, the germanium wafer was rinsed with milli-Q water. In order to prepare the final oxide layer, the Ge sample was dipped in S3 for 30 seconds to remove the oxide layer and then rinsed several times with milli-Q water. The sample is then dipped in S5 for 60 seconds. The Ge wafer was then transferred directly into HPLC grade methanol. A Kimwipe[TM] was used to remove any residual methanol after the sample is removed from the methanol. The sample is then blown gently with dry N_2 gas. Finally, a 0.5% hydrofluoric acid solution was used to etch the germanium surface in order to generate a hydrogen terminated Ge surface. This process took about 20 minutes. if the Ge surface treated dilute hydrofluoric acid solution (0.5%), it has a relatively smoother surface[7,8]. Because H-terminated Ge surfaces will oxidize slowly at atmospheric pressure, the samples were used as soon as possible after preparation and kept under a nitrogen atmosphere.

2.2.3 Surface reaction on the semiconductor surfaces[1,2]

2.2.3.1 Preparation of t-BoC terminated SAM on the Si(100) surface (Figure 2.4)

In this process, the principle that Si-C bonds form the basis of covalently bound monolayers of 1- alkenes on H-terminated Si surfaces is applied. The monolayers have been investigated both experimentally[9-17] and theoretically[18,19].

About 2 mL of t-BoC protected 11-amino-1-undecene was placed into a 30 mL glass vial. After the hydrogen- terminated Si(100) sample was placed into it, the solution was degassed with a dry Ar gas for at least half an hour. Then the vial was immersed in a 90 °C oil bath for 12 hours while maintaining an Ar gas environment. The sample was then removed from the solution and cleaned in diethyl ether, methanol and methylene chloride.

Figure 2.4: Preparation step of 1 t-BoC terminated SAM on Si(100) surface.

2.2.3.2 Preparation of amine terminated SAM on the Si(100) surface (Figure 2.5)

The surface was added to a solution of 25% TFA in methylene chloride for 1 hour. It is followed by a 5 min rinse with 10% NH₄OH solution to remove the t-BoC protecting group and to form the primary amine- terminated surface. The surface was then rinsed with milli-Q water and dried with nitrogen gas.

Figure 2.5: Preparation of amine terminated SAM on the Si(100) surface.

2.2.3.3 Preparation of t-BoC terminated SAM on the Ge(100) surface (Figure 2.6)

About 2 mL of the t-BoC protected 11-amino-1-undecene was placed into a 30 mL glass vial. After the hydrogen- terminated Ge(100) sample was put into it, the solution was degassed with dry Ar gas for at least half an hour. Then the vial was immersed in to 90 $^{\circ}$C oil bath for 12 hours while maintaining an Ar gas environment. Afterward, the sample was removed from the solution and cleaned in diethyl ether, methanol and methylene chloride.
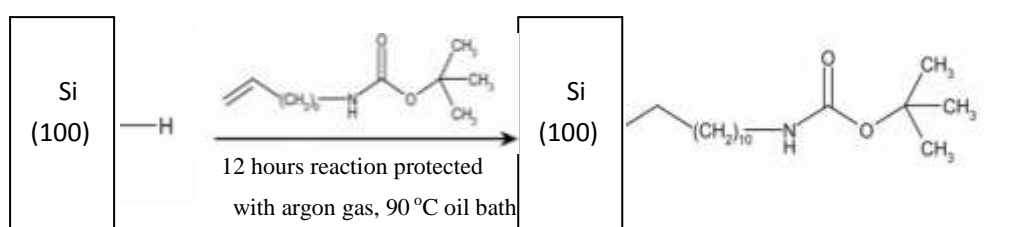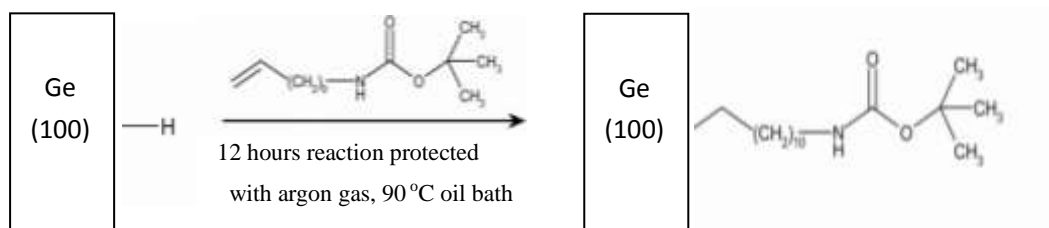

Figure 2.6: Preparation of t-BoC terminated SAM on the Ge(100) surface.

2.2.3.4 Preparation of amine terminated SAM on the Ge(100) surface (Figure 2.7)

The surface was added to a solution of 25% TFA in methylene chloride for 1 hour. It is followed by a 5 min rinse with 10% NH$_4$OH solution to remove the t-BoC protecting group and to form the primary amine- terminated surface. The surface was then rinsed with milli-Q water and dried with nitrogen gas.
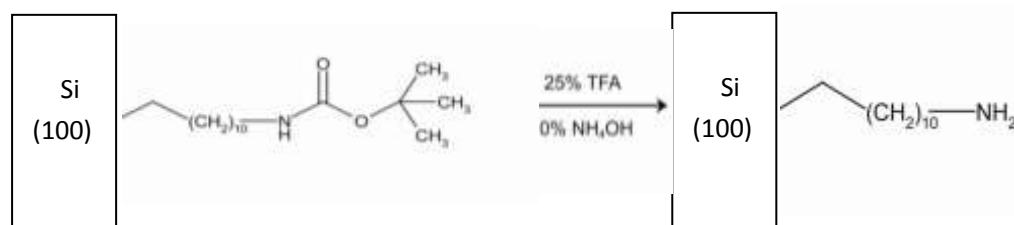

Figure 2.7: Preparation of amine terminated SAM on the Ge(100) surface.

2.2.4   X-ray Photoelectron Spectroscopy Characterization (Figure 2.8)

An x-ray beam irradiates photoelectrons from the surface of the sample you are interested in. The XPS spectrum contains information about only top 1-10 nm of the sample.
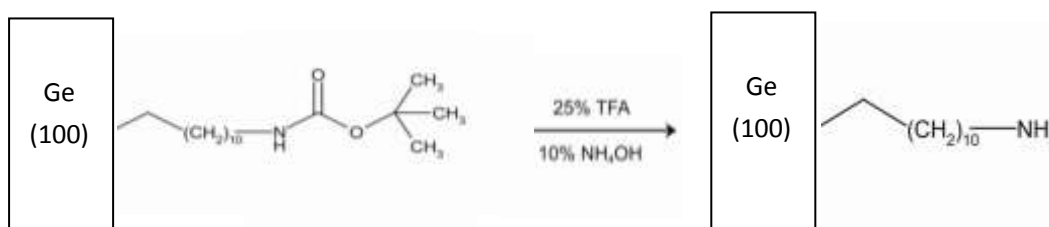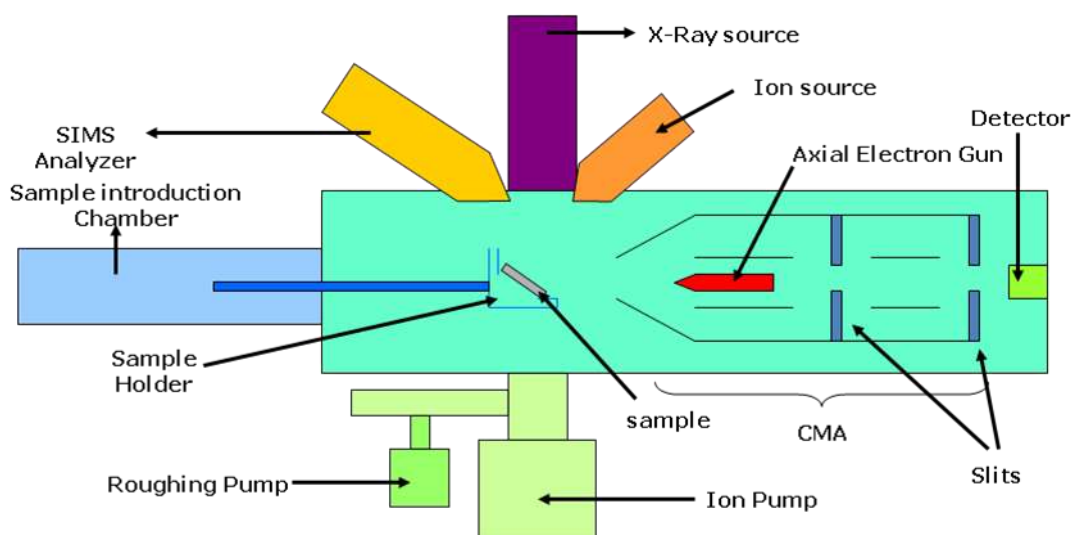

Figure 2.8: Diagram of the Side View of XPS System

2.2.4.1 Experimental information

In this study, XPS was performed using a VSW TA-10 X-ray source with a twin anode (Mg/Al). The Mg K_α anode is operated at 14.5 kV and 20 mA (290 Watts). The Mg K_α photon energy is 1253.6 eV. The Al K_α anode is operated at 14.5 kV and 30 mA (435 Watts). The Al K_α photon energy is 1486.6 eV.

The surface chemistry of on the silicon and germanium (100) substrates was examined in an ultra-high vacuum environment. All experiments were performed in an ultra-high vacuum (UHV) system in order to eliminate the excessive surface

contamination. The base pressure for the system used in this study was 8×10^{-11} torr.

The CMA (Cylindrical Mirror Analyzer) operated is a fixed pass energy mode for XPS to measure the kinetic energy of the emitted electrons. A pass energy of 50 eV was used for high-resolution scans.

2.2.4.2 Quantitative analysis by XPS

$$\frac{n_A}{n_B} = \left(\frac{I_A}{I_B}\right) \times \left(\frac{S_B}{S_A}\right) \times \left(\frac{KE_B}{KE_A}\right)^{0.75} \tag{2.1}$$

In my experiments, equation 2.1 is used to calculate the ratios of elemental concentrations. The intensity value (I) is the peak area of each element detected by XPS. The sensitivity factors (S) for C, N, O, Si and Ge are 1, 1.8, 2.93, 1 and 1 respectively.

2.3 References

1. Zhang, X. C.; Teplyakov, A.V. *Langmuir* **2008**, 24, 810-820.

2. Zhang, X. C.; Kumar, S.; Teplyakov, A.V. *Surf. Sci.* **2009**, 603, 2445-2457.

3. Strother, T.; Cai, W.; Zhao, X.; Hamers, R. J.; Smith, L. M. *J. Am. Chem. Soc.* **2000**, 122, 1205-1209.

4. Wagner, P.; Nock, S.; Spudich, J. A.; Volkmuth. W. D.; Chu, S.; Cicero, R. C.; Wade, C. P.; Linford, M. R.; Chidsey, C. E. D. *J. Struct. Biol.* **1997**,119, 189-201.

5. Hovis, J. S.; Hamers, R. J.; Greenlief, C. M. *Surf. Sci. Lett*, **1999**, 440, 815-819.

6. Prayongpan, P.; Stripe, D. S.; Greenlief, C. M. *Surf. Sci*, **2008**, 602, 571-578.

7. Park, K.; Lee, Y.; Lee, J.; Lim, S. *Appl. Surf. Sci*. **2008**, 254, 1842-1846.

8. Park, K.; Lee, Y.; Lee, J.; Lim, S. *Appl. Surf. Sci*. **2008**, 254, 4828-4832.

9. Linford, M. R.; Fenter, P.; Eisenberger, P. M.; Chidsey, C. E. D. *J. Am. Chem. Soc.* **1995**, 117, 3145-3155.

10. Sieval, A. B.; Demirel, A. L.; Nissink, J. W. M.; Linford, M. R.; van der Maas, J. H.; de Jeu, W. H.; Zuilhof, H.; Sudholter, E. J. R. *Langmuir* **1998**, 14, 1759-1768.

11. Terry, J.; Linford, M. R.; Wigren, C.; Cao, R.; Pianetta, P.; Chidsey, C. E. D. *J. Appl. Phys.* **1999**, 85, 213-221.

12. Buriak, J. M. *Chem. Commun.* **1999**, 1051-1060 and references therein.

13. Sieval, A. B.; Vleeming, V.; Zuilhof, H.; Sudholter, E. J. R. *Langmuir* **1999**, 15, 8288-8291.

14. Boukherroub, R.; Wayner, D. D. M. *J. Am. Chem. Soc.* **1999**, 121, 11513-11515.

15. Strother, T.; Cai, W.; Zhao, X.; Hamers, R. J.; Smith, L. M. *J. Am. Chem. Soc.* **2000**, 122, 1205-1209.

16. Lopinski, G. P.; Wayner, D. D. M.; Wolkow, R. A. *Nature* **2000**, 406, 48-51.

17. Sieval, A. B.; Opitz, R.; Maas, H. P. A.; Schoeman, M. G.; Meijer, G.; Vergeldt, F.J.; Zuilhof, H.; Sudho ̈lter, E. J. R. *Langmuir* **2000**, 16, 10359-10368.

18. Sieval, A. B.; van den Hout, B.; Zuilhof, H.; Sudholter, E. J. R. *Langmuir* **2000**, 16, 2987- 2990.

19. Sieval, A. B.; van den Hout, B.; Zuilhof, H.; Sudholter, E. J. R. *Langmuir* **2001**, 17, 2172- 2181.

Chapter 3: Results and Discussion

X-ray photoelectron spectroscopy (XPS) is used to examine the prepared surfaces on Si(100) and Ge(100). These surfaces include the hydrogen terminated, the t-BoC covered, and the amine terminated surfaces. The XPS results are used to determine the elemental composition of the surfaces and their elemental chemical states. The CasaXPS software package is used to help fit the XPS data and to obtain the corresponding intensities (I) and sensitive factors (S).

3.1 Si(100) samples

XPS is used to monitor the C(1s), N(1s), O(1s), and Si(2p) regions for each of the three prepared surfaces on Si(100). XPS can be used to measure the surface concentrations of these elements and Table 3.1 summarizes these results. The average elemental concentrations are listed in the table with 95% confidence limits. Each of the surfaces were prepared at least three times.   The preparation of the surfaces was reproducible from run to run.

XPS Determined Elemental Surface Concentrations (%)				
Si (100)				
	C	N	O	Si
H/Si	8.1±0.4	1.2±0.1	31.2±1.2	59.5±3.9
t-BoC/Si	33.1±0.8	2.2±0.4	28.1±2.5	36.6±3.5
Amine/Si	30.2±4.5	2.0±0.7	29.0±3.1	38.7±2.5

Table 3.1: Elemental surface concentration (%) as measured by XPS for the hydrogen, t-BoC, and amine terminated Si(100) surfaces

The surface concentrations were determined using equation 2.1, as outlined in the previous chapter. The hydrogen terminated surface has a considerable amount of oxygen and carbon present. The presence of carbon and oxygen is attributed to the amount of time that elapsed between preparation of the surface and the XPS measurement. Hydrogen terminated silicon surfaces are known to have a finite lifetime at atmospheric pressure[1,2] and a native oxide layer is produced over several hours. The hydrogen terminated samples were stored under Ar to help minimize this reaction, but some surface oxidation did occur prior to XPS analysis.

The results for the remaining regions (C(1s), N(1s), and Si(2p)) will be discussed with individual regions that follow. The XPS intensity for a given element varies some from day-to-day due to small changes in X-ray flux and detector settings. To avoid systematic errors, spectra are normalized using relative atomic concentrations so that spectral intensities from different days can be compared directly.

3.1.1 Carbon

The C(1s) region was measured for the hydrogen terminated, t-BOC terminated and amine terminated surfaces. The representative results for these three regions are shown in Figure 3.1. The blue spectrum (lowest curve) shows the results obtained from the hydrogen terminated surface. This residual carbon is most likely due to contamination of the surface while handling it in air at atmospheric pressure. The amount of carbon constitutes about 8% of the surface (from Table 3.1). A similarly hydrogen terminated surface was prepared and immediately reacted with the t-BoC protected compound. The C(1s) spectrum obtained from this surface is shown as the green curve (middle spectrum) in Figure 3.1. The reaction with the t-BoC protected compound results in a larger amount of carbon being observed, consistent with a surface reaction. The C(1s) binding energy also changes and is discussed below. The arrow drawn from the middle spectrum indicates the results of fitting the C(1s) region from the t-BoC terminated surface with the CasaXPS software package. The binding energy scale for the fitted results is compressed compared to the original data in Figure 3.1; so the peaks in the fitted results appear narrower. The red spectrum (top curve) shows the C(1s) results obtained from the amine terminated surface. The C (1s) peak area from the amine terminated surface is about 3% smaller than that obtained from the t-BoC terminated surface. The arrow once again points to the results of fitting the spectrum.
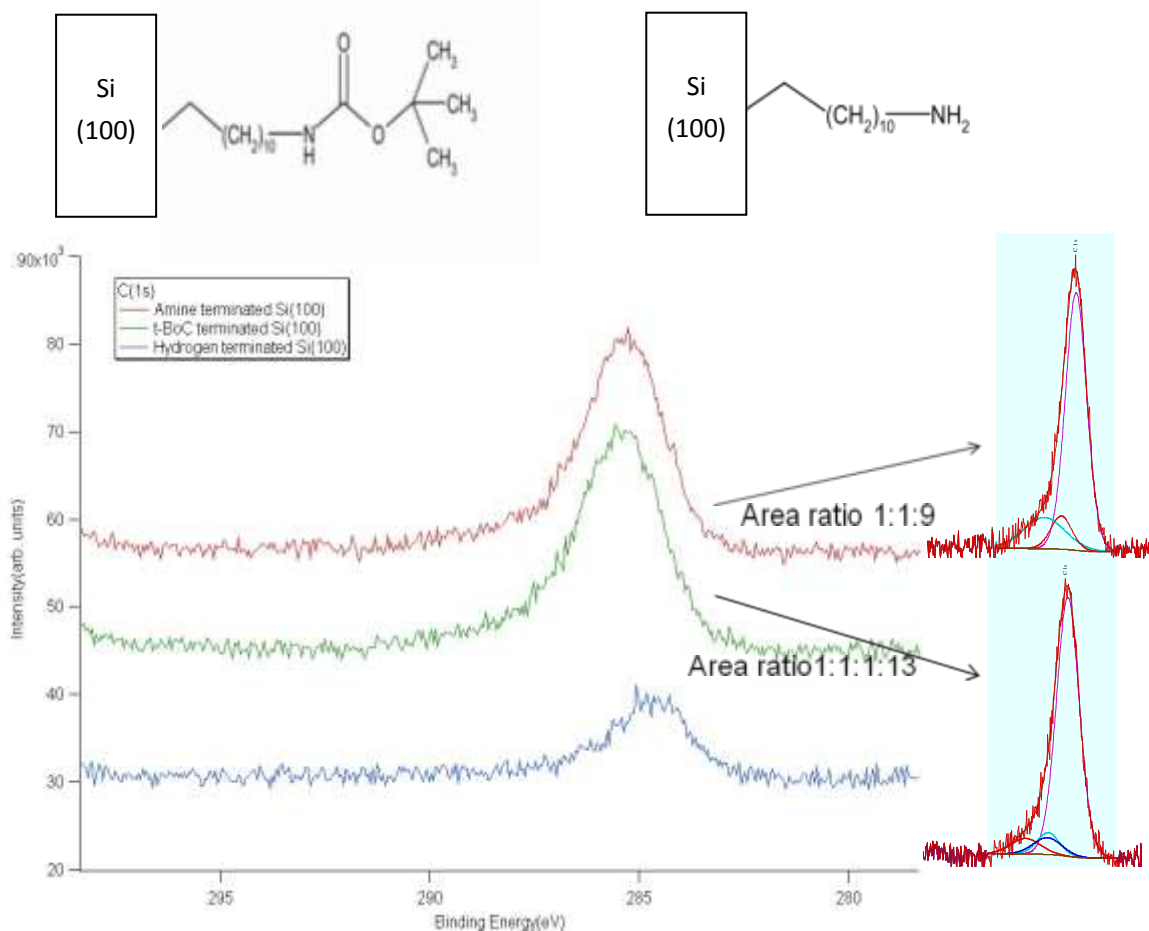
Figure 3.1: C(1s) XPS spectrum of the hydrogen (blue curve), t-BoC (green curve), and amine (red curve) terminated Si(100) surfaces

In an XPS experiment the binding energy (E_B) of an electron is measured. If the electron is from the same element and same electronic energy level, then a binding energy shift can be measured when the element is placed in two different chemical environments. This change in E_B, ΔE_B, is called the chemical shift. Most often, the binding energy shift is measured with respect to the clean atomic surface or the beginning conditions of the surface.

The initial state for a photoemission experiment is the surface (and the

corresponding electronic energy levels) prior to any exposure of X-rays. If the energy of the atom's initial state is changed, then the binding energy (E_B) of the electrons in that atom will change. An example would be the comparison of a neutral atom and its corresponding ion such as Si^0 and Si^{4+}. The change in electronic configuration for such an example is noted in an XPS experiment as an initial state effect. Initial state effects are often responsible for most of a binding energy shift. In the case of Si^0 and Si^{4+}, the higher oxidation state results in a higher binding energy compared to the elemental state because it takes more energy to remove another electron from the cation.

Above Figure 3.1 (left-hand side), the idealized structure of a t-BoC terminated Si(100) sample is shown. There are four kinds of carbon atoms in different chemical environments. The different environments are largely due to the bonding of carbon atoms to atoms with different electron negativities (electron negativity of C, N, O is 2.55, 3.04 and 3.44, respectively[3]. The ratio of the four different kinds of carbon atoms is 1:1:1:13. This expected ratio is consistent with the measured peak area ratios shown in Figure 3.1 for the t-BoC terminated surface.

For amine-terminated Si(100) sample, there are three kinds of carbon atoms in different chemical environments. The ratio of three different carbon atoms is 1:1:9. This ratio is also consistent with the measured peak area ratios shown in Figure 3.1 for the amine terminated surface.

3.1.2 Nitrogen

Figure 3.2 shows the N(1s) XPS spectra for the hydrogen, t-BoC, and amine

terminated Si(100) surfaces. The measured N(1s) peak areas are 3687, 7368, and 7925

for the hydrogen, t-BoC, and amine terminated Si(100) surfaces, respectively. The

presence of residual nitrogen on the hydrogen terminated Si(100) sample indicates

that there is some contamination of the surface from the air. The nitrogen area for the

t-BoC and amine terminated surfaces are approximately the same and are consistent

with the same number of nitrogen atoms present at each surface. The larger measured

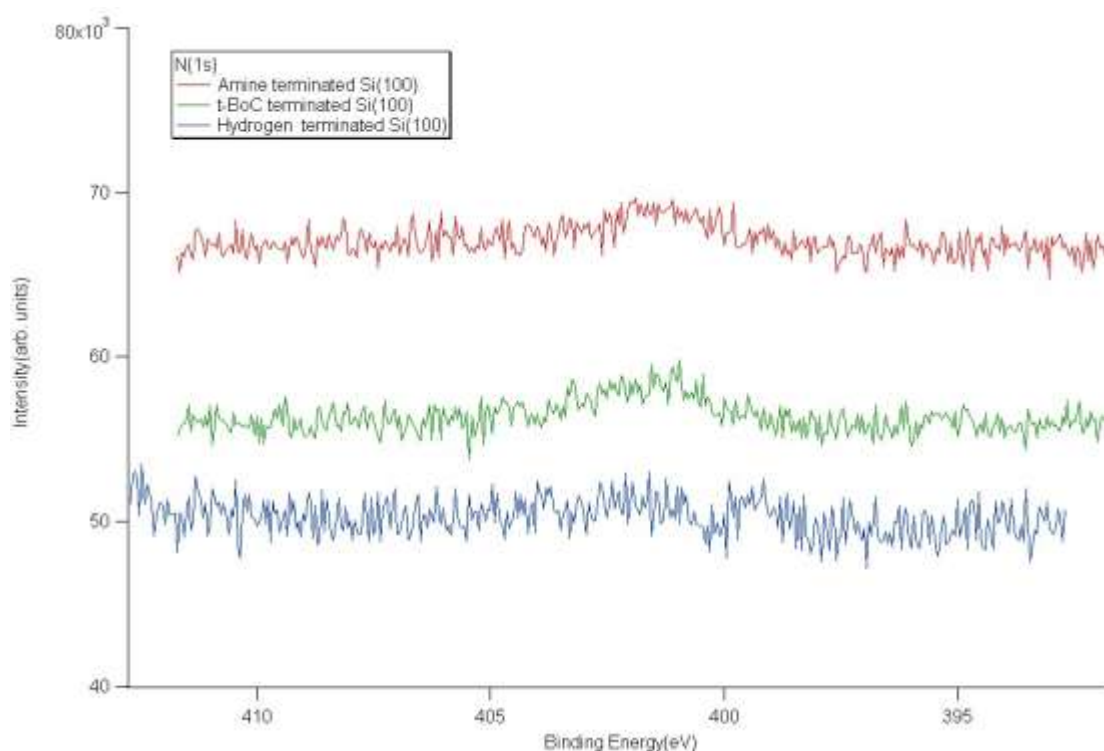area also indicates the addition of a nitrogen-containing species to the surface.

Figure 3.2: N(1s) XPS spectra of the hydrogen (blue), t-BoC (green), and amine
           terminated (red) Si(100) surfaces.

3.1.3 Oxygen

Figure 3.3 shows the O(1s) XPS spectra for the hydrogen, t-BoC, and amine

terminated Si(100) surfaces. In Figure 3.3, the oxygen peak areas for hydrogen, t-BoC, and amine terminated Si(100) surfaces are 141748, 153147 and 157197, respectively. The presence of oxygen in the hydrogen terminated Si(100) sample indicates contamination of the sample between the cleaning step and analysis of the surface. The oxygen areas are higher on the t-BoC and amine terminated surfaces and are the same within the experimental uncertainty. The amount of oxygen present at each of the prepared surfaces will be discussed further in the next section and with the silicon results.
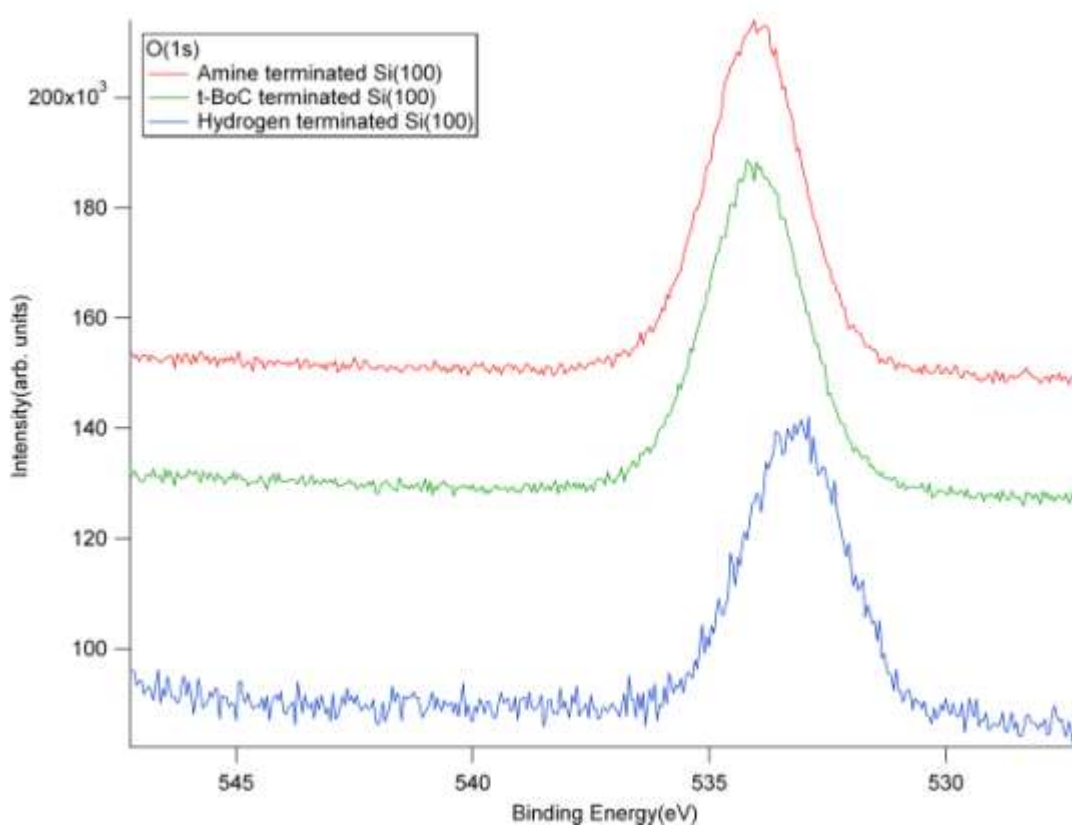

Figure 3.3: O(1s) XPS spectra of the hydrogen (blue), t-BoC (green), and amine terminated (red) Si(100) surfaces.

3.1.4 Silicon

Figure 3.4 shows the Si(2p) XPS spectra for the hydrogen, t-BoC, and amine terminated Si(100) surfaces. A single asymmetric Si(2p) transition is observed for the hydrogen terminated surface, indicating little oxidation of the Si surface. Two photoemission features are observed for the t-BoC and amine terminated Si(100) surfaces at 99.5 eV and 103 eV. The peak at 99.5 eV is the Si(2p) feature for elemental Si, while the peak at 103 eV is characteristic of Si in the 4+ oxidation state. The observation of Si^{4+} is consistent with some of the oxygen measured in Figure 3.3.
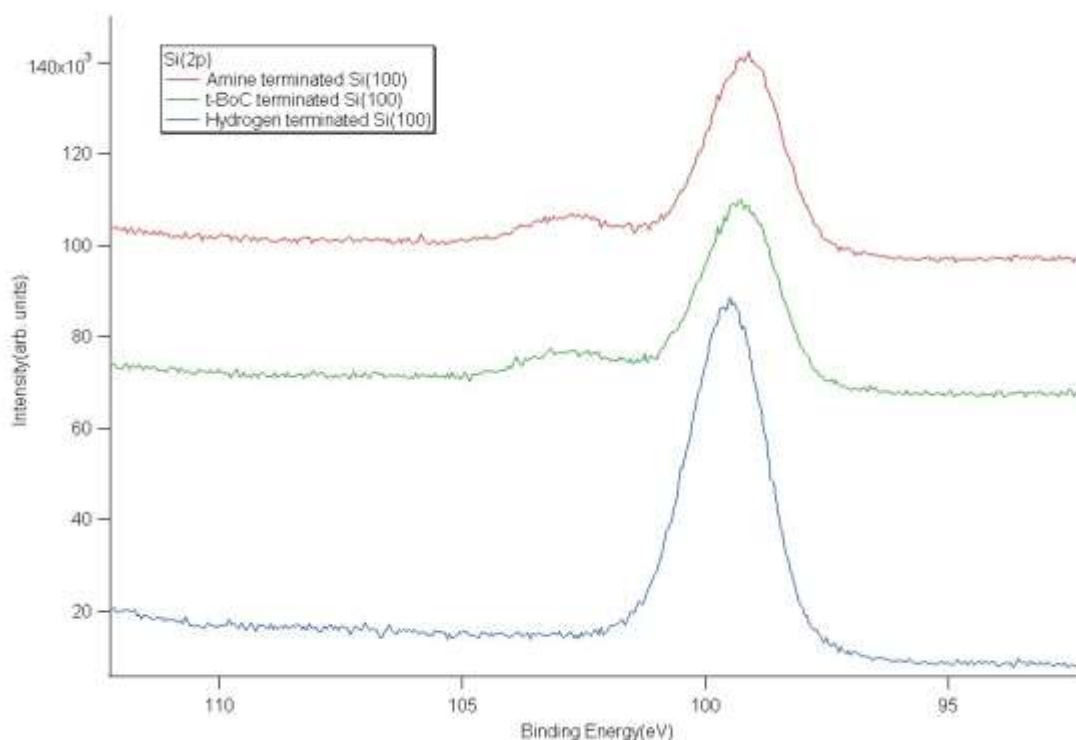

Figure 3.4: Si(2p) XPS spectra of the hydrogen (blue), t-BoC (green), and amine (red) terminated Si(100) surfaces.

3.2 Ge(100) samples

Table 3.1 summarizes the elemental concentrations for the hydrogen, t-BoC, and

amine terminated Ge(100) surfaces. XPS is used to monitor the C(1s), N(1s), O(1s), and Ge(3d) regions for each of the three prepared surfaces on Ge(100). The average elemental concentrations are listed in the table with 95% confidence limits. Each of the surfaces were prepared at least three times. The preparation of the surfaces was reproducible from run to run.

Ge (100)	XPS Determined Elemental Surface Concentrations (%)			
	C	N	O	Ge
H/Ge	6.0±2.8	0.1±0.1	21.5±1.4	72.3±4.2
t-BoC/Ge	38.8±2.9	0.8±0.2	25.9±1.6	34.4±1.0
Amine/Ge	39.3±1.6	1.2±0.3	25.4±1.3	34.1±3.3

Table 3.2: Elemental surface concentration (%) as measured by XPS for the hydrogen, t-BoC, and amine terminated Ge(100) surfaces

The surface concentrations were determined using equation 2.1, as outlined in the previous chapter. The hydrogen terminated surface has a considerable amount of oxygen and carbon present. The presence of carbon and oxygen is attributed to the amount of time that elapsed between preparation of the surface and the XPS measurement. Hydrogen terminated germanium surfaces are known to have a finite lifetime at atmospheric pressure [1,2] and a native oxide layer is produced over several hours. The hydrogen terminated samples were stored under Ar to help minimize this

reaction, but some surface oxidation did occur prior to XPS analysis.

The XPS intensity for a given element varies some from day-to-day due to small changes in X-ray flux and detector settings. To avoid systematic errors, spectra are normalized using relative atomic concentrations so that spectral intensities from different days can be compared directly.

3.2.1 Carbon

Figure 3.5 shows the C(1s) XPS spectra for the hydrogen, t-BoC, and amine terminated Ge(100) surfaces. Comparing with the intensities of carbon peaks in amine and t-BoC terminated Ge(100) samples, a small amount of carbon contamination is observed in hydrogen terminated Ge(100) surface. The residual carbon is most likely due to contamination from air.
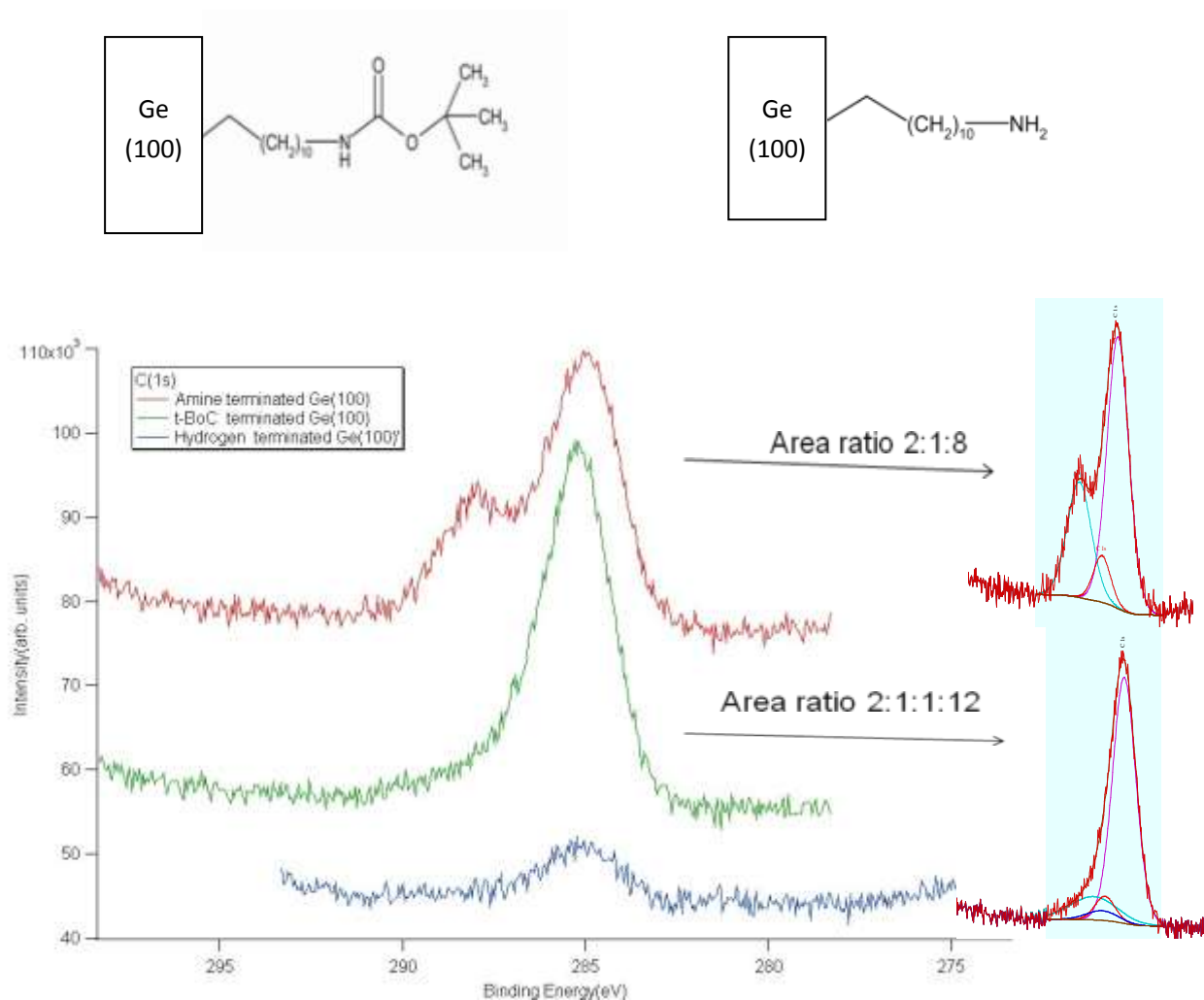
Figure 3.5: C(1s) XPS spectra of the hydrogen (blue), t-BoC (green), and amine (red) terminated Ge(100) surfaces.

In the upper left hand corner of Figure 3.5 is the a drawing of the t-BoC terminated Ge(100) sample. There are four different chemical environments for the carbon atoms, due to the carbon atoms that are linked with atoms of different electron negativity (electron negativity of C, N, O is 2.55, 3.04 and 3.44, respectively). The ratio of the four different kinds of carbon atoms in such a structure is 1:1:1:13. This expected ratio is close the measured peak area ratio of 2:1:1:12 for the t-BoC covered surface.

For the amine terminated Ge(100) sample, there are three kinds of carbon atoms in different chemical environments. The ratio of three different carbon atoms is 1:1:9 for the structure drawn in the upper right hand corner of Figure 3.5. This ratio is roughly consistent with the measured peak area ratio of 2:1:8.

3.2.2 Nitrogen

Figure 3.6 shows the N(1s) XPS spectra for the hydrogen, t-BoC, and amine terminated Ge(100) surfaces. In Figure 3.6 the nitrogen peak areas for the hydrogen, t-BoC, and amine terminated Ge(100) surfaces are 3444, 3492 and 5204, respectively. Thus, the conclusions that the presence of nitrogen residual in the hydrogen terminated Ge(100) sample may come from air or chemical contamination could be drawn from it. The measured nitrogen peak area of the amine terminated Ge(100) surface is slightly greater than that in t-BoC terminated Ge(100) surface. However, the atomic concentration of nitrogen is the same for the two surfaces as indicated in Table 3.2.
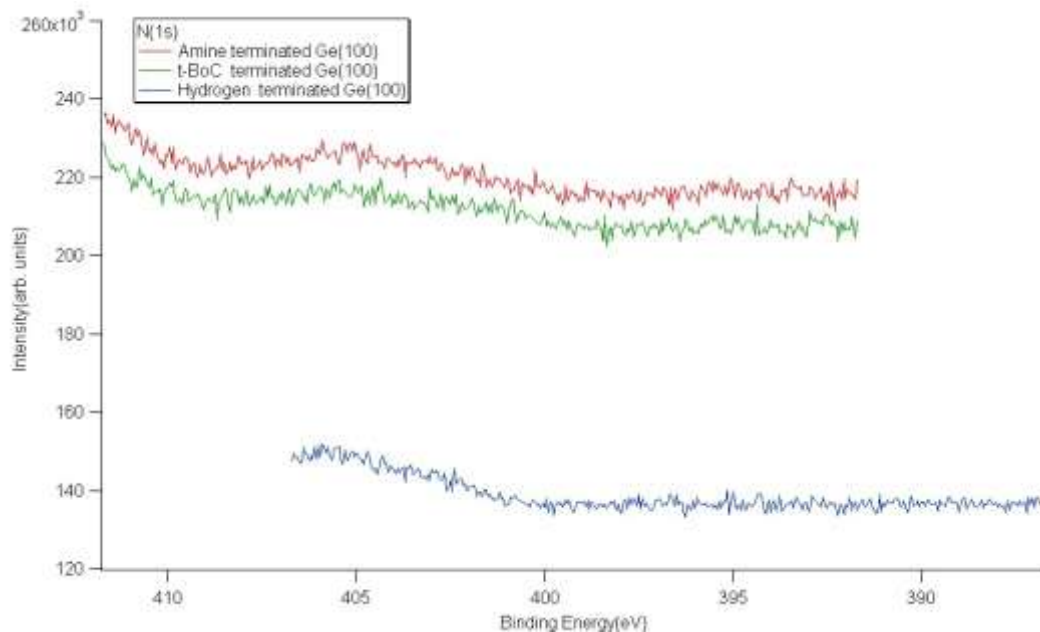
Figure 3.6: N(1s) XPS spectra of the hydrogen (blue), t-BoC (green), and amine (red) terminated Ge(100) surfaces.

3.2.3 Oxygen

Figure 3.7 shows the O(1s) XPS spectra for the hydrogen, t-BoC, and amine terminated Ge(100) surfaces. In Figure 3.7 the oxygen peak areas for the hydrogen, t-BoC, and amine terminated Ge(100) surfaces are 132778, 186819 and 184564, respectively. The presence of oxygen in the hydrogen terminated Ge(100) sample is most likely due to air contamination. Based on the oxygen percentage in molecular formula, the oxygen content in amine terminated Ge(100) surface is slightly lower than that for the t-BoC terminated Ge(100) surface, consistent with removal of the t-BoC group. The broadening of the O(1s) peak for both the amine and t-BoC terminated surfaces indicates the presence of oxygen in at least two different chemical environments. One of the oxygen environments is similar to that observed for the

68

hydrogen terminated surface and is assigned to surface contamination. The second environment is to the higher binding energy side and will be discussed further in the following section.
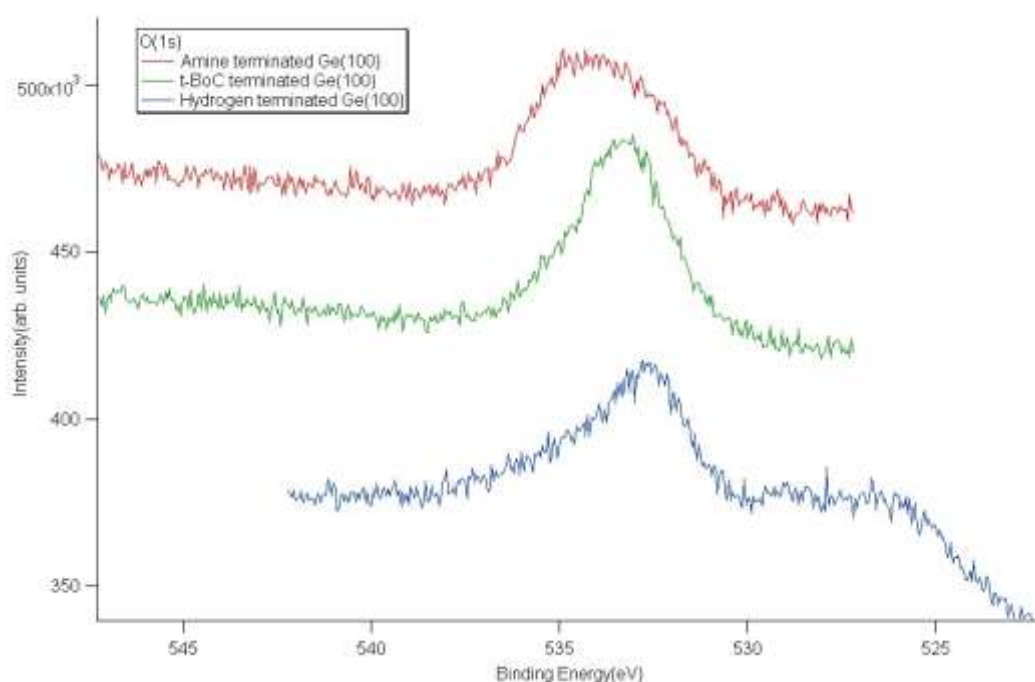

Figure 3.7: O(1s) XPS spectra of the hydrogen (blue), t-BoC (green), and amine (red) terminated Ge(100) surfaces.

3.2.4 Germanium

Figure 3.8 shows the Ge(3d) XPS spectra for the hydrogen, t-BoC, and amine terminated Ge(100) surfaces. The hydrogen terminated surface (lower blue spectrum) shows a single Ge(3d) transition. The intensity of the peak is larger than the other two spectra consistent with the surface not containing an organic surface layer. The Ge(3d) spectra from the t-BoC and amine terminated surfaces contain two photoemission features at about 29 eV and 32eV. The peak at 29 eV is Ge(3d) XPS spectrum of

69

elemental Ge and is the same as that observed for the hydrogen terminated surfaces.

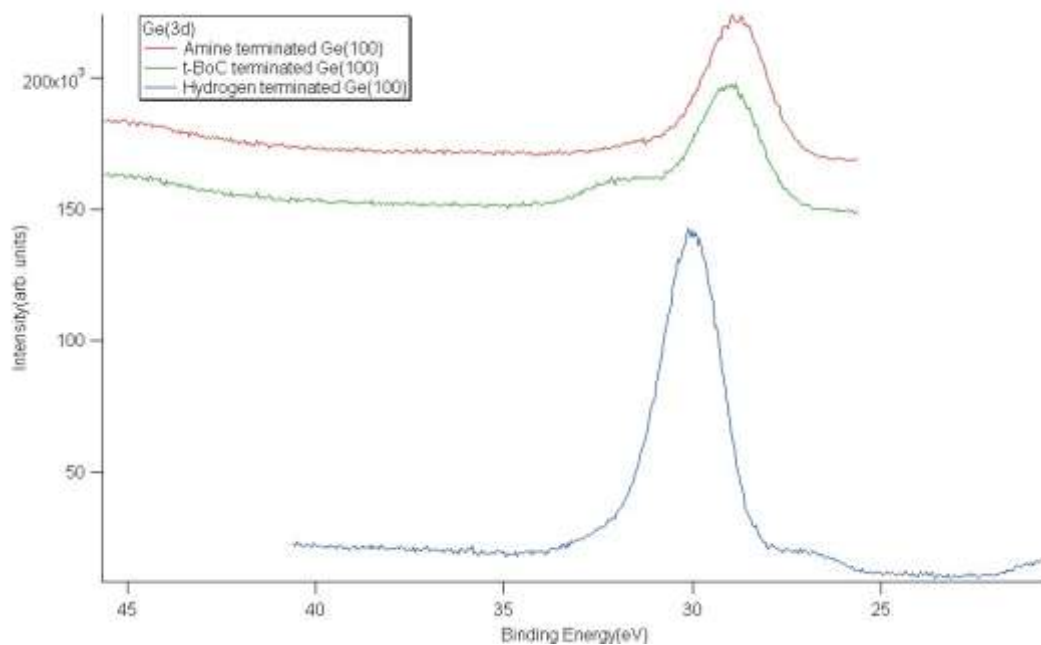The second peak is observed at 32 eV and is consistent with the presence of some

GeO$_2$.

Figure 3.8: Ge(3d) XPS spectra of the hydrogen (blue), t-BoC (green), and amine (red) terminated Ge(100) surfaces.

3.3 References

1. Deegan, T.; Hughes, G. *Appl. Surf. Sci.* **1998**. 123/124:66–70.

2. Rivillon, S.; Chabal, Y. *Appl. Phys. Lett.* **2005**, 87, 253101

3. Dean, J. A. (ed) *Lange's Handbook of Chemistry* (15th Edition), McGraw-Hill, 1999; Section 4; Table 4.5, Electronegativities of the Elements.

Chapter 4: Conclusions

The attaching method of t-butyloxycarbonyl (t-BoC)-protected 11-amino-1-undecene on Si(100) and Ge(100) surfaces was examined in my research. After certain wet chemical treatment, Si(100) and Ge(100) surfaces can be covered with 11-amino-1-undecene for the first time.

X-ray photoelectron spectroscopy (XPS) is used to analyze the hydrogen, t-BoC, and amine terminated Si(100) or Ge(100) surfaces. Then elemental percentages of carbon, nitrogen, oxygen and silicon/ germanium on a semiconductor surface were identified. Based on the analysis by Software CasaXPS, the elemental concentration percentages with 95% confidence limits of the mean values can testify the reproducibility and reliability of the procedure for coupling t-BoC protected 11-amino-1-undecene and removing t-BoC group. Besides, the procedure is very easily operated. Thus, the procedure for coupling t-BoC protected 11-amino-1-undecene and removing t-BoC group is very straightforward and reliable.

Future experiments might include coupling reactions at the amine group of amine terminated semiconductor surfaces. This will help to develop gold ion probes to assess the quantity of environmental gold ions by luminescence methods.

VITA

Jing Liu was born in June, 1982 in Hebei Province, P. R. China. She obtained a B.S. in Environmental Engineering from North China Electric Power University, Hebei Province in 2005 and a M.S. in Environmental Science and Engineering from North China Electric Power University, Hebei Province in 2008.

Her research focused on the procedure development of attaching 11-amino-1-undecene on Si(100) and Ge(100) surfaces and X-ray photoelectron spectroscopy (XPS) examination of 11- amino-1-undecene covered Si (100) and Ge (100) surfaces. She received a M. S. in Chemistry from University of Missouri-Columbia in 2011.